HALL EFFECT INVESTIGATIONS IN n-InSb UNDER PRESSURE

by

SIN-MIN FONG

A Thesis Submitted in Partial Fulfillment of the Requirements for the

DEGREE OF MASTER OF SCIENCE

DEPARTMENT OF PHYSICS
LAKEHEAD UNIVERSITY
THUNDER BAY, ONTARIO, CANADA
JULY, 1978

ProQuest Number: 10611614

All rights reserved

INFORMATION TO ALL USERS
The quality of this reproduction is dependent upon the quality of the copy submitted.

In the unlikely event that the author did not send a complete manuscript
and there are missing pages, these will be noted. Also, if material had to be removed,
a note will indicate the deletion.

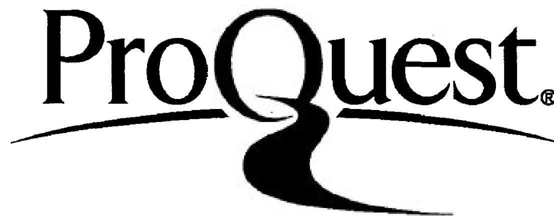

ProQuest 10611614

Published by ProQuest LLC (2017). Copyright of the Dissertation is held by the Author.

All rights reserved.
This work is protected against unauthorized copying under Title 17, United States Code
Microform Edition © ProQuest LLC.

ProQuest LLC.
789 East Eisenhower Parkway
P.O. Box 1346
Ann Arbor, MI 48106 - 1346

THESES
M.Sc.
1978
F67
c.1

Copyright (c) Sin Min Fong 1978

268055

ACKNOWLEDGEMENTS

It gives me great pleasure to thank Dr. W.J. Keeler, my research supervisor for his generous and instructive assistance throughout this project.

Special thanks are due to Professor M. Hawton for her helpful discussions concerning the data analysis and to Dr. R.E. Jones for his interest in the project.

I wish to express my appreciation to Mr. G.C. Anderson for machining the pressure vessel parts, and helping to maintain the cryostats.

The cooperation from my colleague, Mr. N.U. Ahmad, in using the apparatus is greatly appreciated.

I also wish to thank my wife for her constant encouragement throughout this work.

Finally, I wish to thank Mrs. J. Boucher for typing the thesis.

TABLE OF CONTENTS

		Page
List of Figures		*i*
Abstract		1
Introduction		2
Chapter 1.	Theoretical Considerations	5
1-1	Band Structure in InSb	5
1-2	Low Electric Field Properties of Intrinsic Semiconductors	9
1-3	Low Electric Field Properties of Extrinsic Semiconductors	11
1-4	Scattering Processes and Mobility	13
1-4(I)	High Temperature Case	13
1-4(II)	Low Temperature Case	15
1-5	Hall Effect Measurements and the van der Pauw Technique	16
Chapter 2.	Equipment and Sample Preparation	20
2-1	The Pressure Vessel	20
2-2	Sample Preparation	20
2-3	Experimental Methods	22
Chapter 3.	Results and Discussions	25
3-1	Constant Temperature Variable Pressure Results	25
3-2	Constant Pressure Variable Temperature Results	25
3-3	Temperature and Pressure Dependence of the Hall Mobility	31
3-3(a)	Temperature Dependence	31

Page

3-3(b)	Pressure Dependence (77K-300K)	34
3-4	Pressure Dependence of the Donor gap E_D	39
3-5	Pressure Dependence of the Intrinsic gap E_g	47
Chapter 4.	Conclusions	51
References		53

LIST OF FIGURES

Figure		Page
1	Band structure of InSb.	6
2	Arrangement for specific resistivity measurements.	17
3	Arrangement for Hall measurements.	19
4	The pressure vessel.	21
5a	Resistivity ρ vs P for n-InSb at T = 296K.	26
5b	Resistivity ρ vs P for n-InSb at T = 198K, 77K.	27
6a	Carrier concentration n vs P for n-InSb at T = 296K.	28
6b	Carrier concentration n vs P for n-InSb at T = 198K, 77K.	29
7	Mobility μ vs P for n-InSb at T = 296K, 198K, 77K.	30
8	Mobility μ vs T for n-InSb at different pressures.	32
9	Resistivity ρ vs T for n-InSb at different pressures.	33
10	Mobility μ vs intrinsic gap E_g for n-InSb at T = 296K, 198K, 77K.	35
11a	$n^2/(N_D-n)T^{3/2}$ vs 1/T for n-InSb at P = 4.4 kbar, 8.1 kbar, 9.7 kbar. N_D is the donor concentration.	40
11b	$n^2/(N_D-n)T^{3/2}$ vs 1/T for n-InSb at P = 11 kbar, 12.6 kbar. N_D is the donor concentration.	41
12	Donor gap E_D vs pressure P for n-InSb.	43
13	Electrical conductivity $\sigma(T)$ vs 1/T for n-InSb at P = 0.2 kbar, 2.75 kbar, 5.0 kbar, 7.5 kbar, 9.74 kbar.	46
14	Zero temperature intrinsic gap E_{go} vs pressure P for n-InSb.	49

ABSTRACT

Low field electrical transport properties of n-InSb in the temperature range 6.4K-300K have been studied under pressures up to 15 kbar using Hall measurements. The pressure dependence of the carrier concentration, the intrinsic gap and the extrinsic gap have been studied. The extrinsic gap, E_D, is found to increase approximately exponentially with increasing pressure. This is responsible for carrier freeze-out under pressure. The scattering process at temperatures above 100K is dominated by a combination of polar optical and electron-hole scattering while at temperatures below 40K it is dominated by neutral impurity and ionized impurity scattering.

INTRODUCTION

InSb is a small gap semiconductor with interesting and widely varying properties. In the extrinsic region a thorough understanding of the impurity levels is essential. In recent years there has been considerable activity by both experimentalists[1-6] and theoreticians[7] in this area, and in n-InSb in particular there are still different points of view about the existence of a donor band and how its levels are influenced by magnetic fields, temperature, electric fields and other parameters. A study of the behavior of these donor levels under pressure can be very useful because of the relatively large effect pressure has on InSb (for example, 12 kbar doubles E_g).

Long[8] performed measurements on the effect of pressure on the resistivity and Hall coefficient in the intrinsic region for pressures up to 2 kbar. He found a value of $\frac{dE_g}{dP}$ of 14.2 meV/kbar. Keyes[9] performed a measurement on the pressure dependence of the resistivity at pressures up to 12 kbar and temperatures above 200K. His value of $dE_g/dP \approx 15$ meV/kbar is somewhat higher.

Electrical investigation of the donor states in InSb has been carried out in the presence of high magnetic fields and to a lesser degree under pressure. Sladek[1] measured the electrical resistivity and Hall coefficient for "pure" (undoped) n-type material for a magnetic field up to 30kOe and a wide temperature range. At 4.2K the Hall coefficient increased sharply with increasing magnetic field. He concluded that impurity levels were initially merged with the conduction band and that the magnetic field separated them. On the

other hand, other workers[3,6] assert that there is always an impurity gap of 0.2-0.5 meV at T = 4.2K and H = 0 and that this value changes with the magnetic field.

Porowski and various co-workers[10,11] have been primarily responsible for the limited existing pressure studies on donor states in n-InSb. They report an anomalous behavior in the Hall coefficient for the high temperature extrinsic region (90K-140K) and try to analyze this in terms of a combination of shallow and deep donor levels whose existence they attribute to donors occupying two different crystallographic sites in the crystal. Much of their work is centered on this "anomaly".

The temperature dependence and pressure dependence of the electron mobility are of interest because the mobility reflects the dominant scattering mechanisms in the different regimes. Little has been reported on the pressure dependence of the electron mobility since most pressure work has not been of the Hall type.

While the low electric field properties of InSb are interesting in their own right, high electric field Gunn investigations on n-InSb have shown two different behavior patterns with the application of pressure. Either the Gunn threshold electric field decreases monotonically with increasing electric field for pressures up to 15 kbar, or it shows a minimum at about 9 kbar and then increases and weakens as pressure increases to about 12 kbar. The difference in these two behavior patterns is thought to be due to carrier freeze-out for the

latter case and not for the former.

Since undoped n-InSb shows such a variety of effects and since many of these are strongly pressure dependent and still incompletely understood, it was decided that both the Gunn effect and the low field transport properties would be studied in n-InSb under pressure. While the Gunn effect study was carried out primarily at 77K, the Hall and conductivity investigations were carried out between room temperature and 6.4K. This thesis reports primarily on the low field transport work, however, reference to the Gunn effect study is made after the results on the donor gap are obtained.

In chapter 1, we shall briefly discuss the band structure of InSb, low electric field intrinsic and extrinsic behaviors and scattering processes in a parabolic band approximation. The van der Pauw method is discussed. Equipment and sample preparation are considered in chapter 2. In chapter 3 results and discussions are presented. Chapter 4 presents the conclusions.

Chapter 1

Theoretical Considerations

1-1. Band Structure in InSb.

A reasonable amount of reliable band structure information is available for InSb.

The lowest energy conduction and valence band extrema in InSb are located around $\vec{K} = 0$. The conduction band consists of two sub-bands and the minimum of the lowest conduction band lies at the center of the Brillouin zone (Γ point) at which the band has the largest curvature (i.e., the smallest electron effective mass). For low energies it is parabolic, however, it deviates from parabolicity at energies of only several hundredths of an electron volt up from the bottom of the band for zero pressure. The band structure of InSb is shown in Fig. 1. The energy difference between Γ and L conduction band edges, $E_{\Gamma L}$, is over twice the valence band to conduction band gap at $\vec{K} = 0$ and $P = 0$.

Kane[12] has performed a detailed calculation of the band structure for small band gap semiconductors such as InSb and InAs. With two parameters p, the interband interaction matrix element and Δ, the spin-orbit splitting energy at $\vec{K} = 0$, he obtained the following $E - \vec{K}$ relations for the conduction band and the valence bands. For the conduction band (energy measured from the top of the valence band)

$$E = E_g + \frac{\hbar^2 K^2}{2m_0} + \frac{1}{2}\left[\left(E_g{}^2 + \frac{8p^2K^2}{3}\right)^{1/2} - E_g\right]$$

Figure 1. The band structure of InSb at T=0 K.
The dashed curves show the bands under a pressure of approximately 15 kbar.

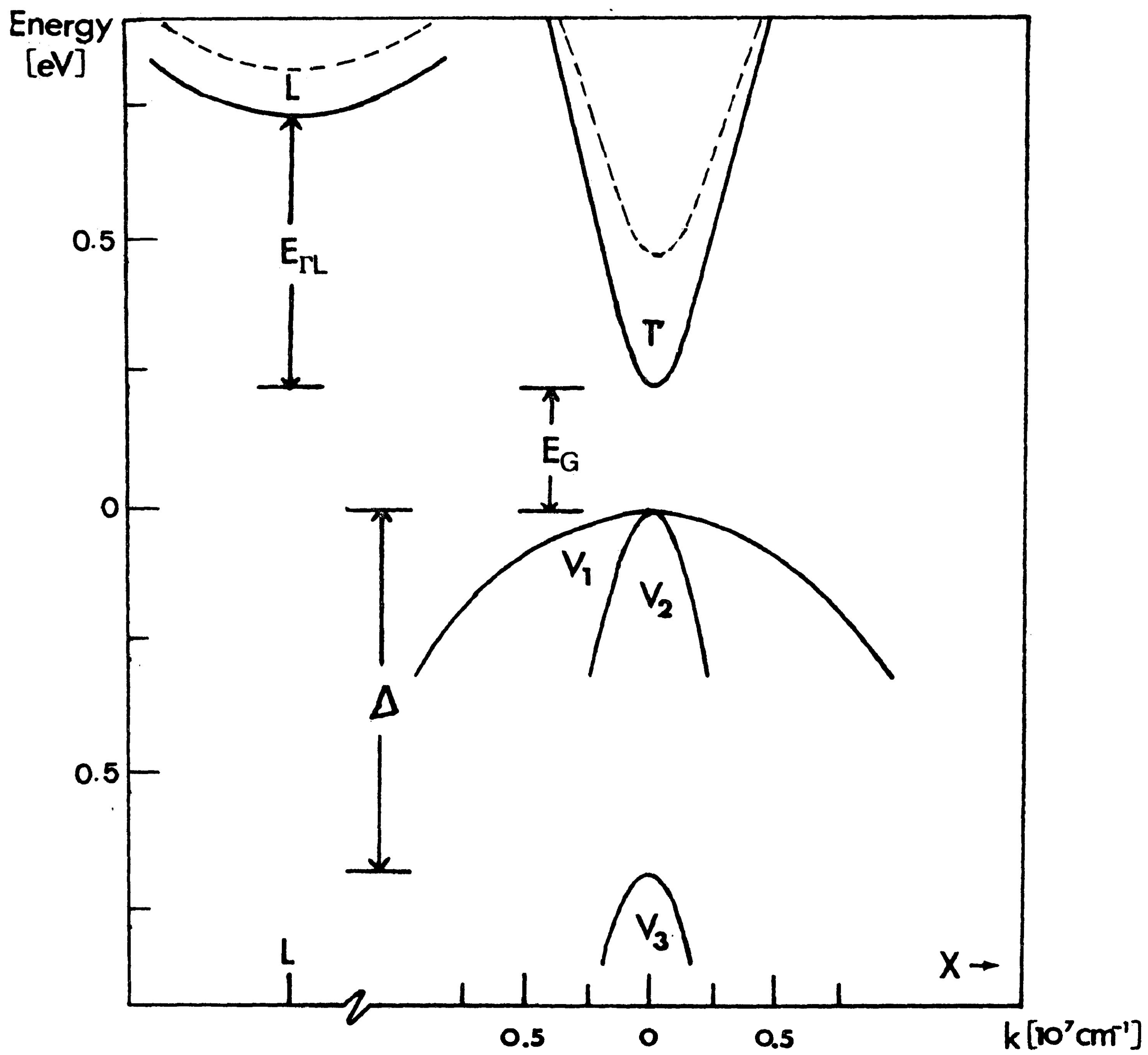
Energy
[eV]
L
0.5
$E_{\Gamma L}$
Γ
E_G
0
V_1
V_2
Δ
0.5
V_3
L
X →
0.5
0
0.5
k [10^7 cm^{-1}]

For the valence bands (energy measured from the top of the valence band)

$$E = -\frac{\hbar^2 K^2}{2m_o} \qquad \text{heavy hole band}$$

$$E = -\frac{\hbar^2 K^2}{2m_o} - \frac{1}{2}\left[\left(E_g^{\,2} + \frac{8p^2K^2}{3}\right)^{\frac{1}{2}} - E_g\right] \qquad \text{light hole band}$$

$$E = -\Delta - \frac{\hbar^2 K^2}{2m_o} - \frac{p^2K^2}{3(E_g+\Delta)} \qquad \text{spin-orbit split band}$$

where m_o is the free electron mass and E_g is the valence to conduction band gap. The parameter Δ appears only in the expression for the split-off valence band. If energy E' is measured from the bottom of the conduction band and the term $\hbar^2K^2/2m_o$ is ignored (since $m_o \approx 80m_n^*$ in the conduction band) the conduction band may be represented by

$$E' = \frac{1}{2}\left[\left(E_g^{\,2} + \frac{8p^2K^2}{3}\right)^{\frac{1}{2}} - E_g\right] \qquad (1\text{-}1\text{-}1)$$

Defining m_n^* as $m_n^* = \frac{3\hbar^2 E_g}{4p^2}$ and substituting it into equation (1-1-1) to eliminate p^2 one obtains

$$\frac{\hbar^2K^2}{2m_n^*} = E'\left(1 + E'/E_g\right) \quad , \qquad (1\text{-}1\text{-}2)$$

which is a hyperbolic relation between E' and $\vec{K}$. Provided the conduction band is not too full ($E' << E_g$) equation (1-1-2) reduces to a parabolic relation between E' and K given by

$$E' = \frac{\hbar^2K^2}{2m_n^*} \qquad (1\text{-}1\text{-}3)$$

Pressure increases the gap E_g and hence the electron effective mass m_n^*. Since the density of states in a parabolic band is proportional to $m^{3/2}$, increasing pressure improves the parabolic band assumption both through a larger available density of states and E'/E_g variation.

The L conduction band edge is estimated to lie between 0.42 and 0.52 eV above the bottom of the L conduction band. Estimates of pressure derivatives for E_g and $E_g + E_{\Gamma L}$ are[8,9,13] 14 x 10^{-3} eV/kbar and 8.3 x 10^{-3} eV/kbar respectively. Thus $E_{\Gamma L}$ should decrease with increasing pressure at about -6 x 10^{-3} eV/kbar. This effect along with the fact that $\mu_\Gamma >> \mu_L$ leads to negative differential conductivity and the Gunn effect in n-InSb under pressure and high electric field.

Since $E_g < E_{\Gamma L}$, avalanche pair production normally occurs in preference to Γ to L band electron transfer when a large electric field is applied. Thus, the Gunn effect occurs for only about 1 nanosecond at P = 0 before avalanching obliterates it. However, since E_g increases and $E_{\Gamma L}$ decreases for increasing pressure, the Gunn effect may be stabilized in n-InSb when pressure is increased.

The valence bands V_1 and V_2 are degenerate at $\vec{K} = 0$, however, the hole density of states is determined primarily by the low curvature, low mobility heavy hole band, V_1. For low electric field studies the split-off band V_3 does not contribute.

1-2. Low Electric Field Properties of Intrinsic Semiconductors

The number of electrons per unit volume in a parabolic conduction band for an intrinsic semiconductor is given by

$$n = N_c \mathcal{F}_{\frac{1}{2}}(\eta) \qquad (1\text{-}2\text{-}1)$$

where $N_c = 2(2\pi m_n^* K_B T/h^2)^{3/2}$ is referred to as the "effective density of states in the conduction band," and m_n^* is the electron effective mass.

$$\mathcal{F}_{\frac{1}{2}}(\eta) = \frac{2}{\pi^{\frac{1}{2}}} \int_{E_c=0}^{\infty} \frac{\varepsilon^{\frac{1}{2}} d\varepsilon}{1+\exp(\varepsilon-\eta)} \qquad (1\text{-}2\text{-}2)$$

is the Fermi-Dirac integral, and $\varepsilon = \frac{E-E_c}{K_B T}$, $\eta = \frac{E_f-E_c}{K_B T}$. A similar expression exists for the density of holes p in a parabolic valence band.

The densities n and p in an intrinsic semiconductor depend only on the nature of the conduction and valence band, the intrinsic energy gap between them, E_g, and temperature T.

For a semiconductor such as InSb with a small intrinsic energy gap ($E_g \approx 0.2$ eV) intrinsic behavior becomes dominant at temperatures above $\sim$ 150 K.

In the intrinsic case electrical neutrality requires that $n = p = n_i$, the intrinsic carrier concentration, and this sets the position of the Fermi level.

In a non-degenerate intrinsic case, that is, when the intrinsic energy gap is a fairly large multiple of $K_B T$ and the masses m_n^*, m_p^*

are not too dissimilar, n_i is small compared with both N_c and N_v. Then the Fermi integrals can be replaced by their non-degenerate limiting forms, so that

$$n = 2(2\pi m_n^* K_B T/h^2)^{3/2} \exp\left(\frac{E_f - E_g}{K_B T}\right) \qquad (1\text{-}2\text{-}3)$$

and

$$p = 2(2\pi m_p^* K_B T/h^2)^{3/2} \exp\left(-\frac{E_f}{K_B T}\right) . \qquad (1\text{-}2\text{-}4)$$

The intrinsic carrier concentration n_i can be obtained from the law of mass action

$$n_i = (np)^{1/2} = 2(2\pi K_B T/h^2)^{3/2}(m_n^* m_p^*)^{3/4} \exp\left(-\frac{E_g}{2K_B T}\right) . \qquad (1\text{-}2\text{-}5)$$

By setting equations (1-2-3) and (1-2-5) equal, one obtains the Fermi level

$$E_f = \frac{1}{2} E_g + \frac{3}{4} K_B T \log(m_p^*/m_n^*) \qquad (1\text{-}2\text{-}6)$$

which is temperature dependent. If $m_n^* = m_p^*$, then the Fermi level is temperature independent and lies in the middle of the gap.

The exponential term in equation (1-2-5) provides most of the temperature dependence for n_i, even though the coefficient of the exponential varies as $T^{3/2}$. For completeness one should plot $\ell n(n_i/T^{3/2})$ vs $(\frac{1}{T})$ to determine E_g.

For temperatures above 200K, E_g is usually assumed to vary with temperature as

$$E_g = E_{go} - \alpha T \quad (1\text{-}2\text{-}7)$$

Substituting (1-2-7) into (1-2-5) one obtains

$$n_i = 2(2\pi K_B T/h^2)^{3/2}(m_n^* m_p^*)^{3/4} \exp(\alpha/2K_B) \exp\left(-\frac{E_{go}}{2K_B T}\right)$$

or

$$\frac{n_i}{T^{3/2}} = 2(2\pi K_B/h^2)^{3/2}(m_n^* m_p^*)^{3/4} \exp \frac{\alpha}{2K_B} \exp\left(-\frac{E_{go}}{2K_B T}\right) \quad (1\text{-}2\text{-}8)$$

Stated this way, a semilog plot of $n_i/T^{3/2}$ vs $(1/T)$ yields a value of the gap E_{go} for T = 0K, not the gap at the temperature of the measurements.

1-3. Low Electric Field Properties of Extrinsic Semiconductors

Analogous to the derivation for n in the intrinsic case, an expression for the density of carriers n in a parabolic conduction band for the extrinsic case can be obtained.

For high temperatures (temperatures above about 80K for n-InSb) where the donors are totally ionized,

$$n = N_D = N_c \exp\left(\frac{E_f - E_g}{K_B T}\right) \quad (1\text{-}3\text{-}1)$$

For low temperatures

$$n = (N_D N_C)^{1/2} \exp\left(-\frac{E_D}{2K_B T}\right) \quad (1\text{-}3\text{-}2)$$

where $N_c = 2(2\pi m_n^* K_B T/h^2)^{3/2}$ is the effective density of states in the parabolic conduction band, N_D is the number of donors per unit volume and E_D is the energy gap between the donor level and the conduction band.

However, an analysis of carrier concentration in the low temperature extrinsic limit is complicated by the possible effects due to a low concentration of acceptors and the resulting compensation. Seeger[14] has given a treatment of this problem and provided one is in the non-degenerate case which is true for pressures greater than ~5 kbar in InSb

$$\frac{n(n+N_A)}{N_D-N_A-n} = \frac{N_c}{g_D} \exp\left(-\frac{E_D}{K_B T}\right) \qquad (1\text{-}3\text{-}3)$$

Here N_A is the number of acceptors per unit volume and g_D accounts for possible multiplicity in atom bound states.

In the case of a "pure", that is undoped sample, impurity scattering is low and there is little compensation. Also, $N_A \ll N_D$ and provided n is not too small, N_A may be neglected in the numerator in equation (1-3-3). This leaves

$$\frac{n^2}{N_D-n} = \frac{N_c}{g_D} \exp\left(-\frac{E_D}{K_B T}\right) \qquad (1\text{-}3\text{-}4)$$

Since N_c is proportional to $T^{3/2}$ for a parabolic conduction band limit, a semilog plot of $\frac{n^2}{(N_D-n)T^{3/2}}$ vs $\frac{1}{T}$ should be temperature independent, provided the assumed Boltzman statistics apply.

The expression (1-3-4) provides one with information about the donor gap E_D at different pressures, since carrier de-ionization across a donor gap is responsible for the decrease of n with decreasing temperature and/or increasing pressure.

1-4. Scattering Processes and Mobility

Carriers travelling through a crystal at temperatures above absolute zero have their mobility limited by several scattering mechanisms. A brief review of the most important of these is given below. These mechanisms fall roughly into two temperature regions with 50-80K as the demarcation between high and low temperature behavior.

(I) High Temperature Case

(a) Acoustic Phonon Scattering.

One possible interaction that limits carrier drift velocity at high temperatures is the interaction with acoustic lattice vibrations (acoustic phonons). Bardeen and Shockley[15] have shown that the acoustic phonons limit the carrier mobility to

$$\mu_A = 3.2\times10^{-5}\rho u^2 \left(\frac{m_o}{m_n^*}\right)^{5/2} \Big/ T^{3/2} E_1^{\,2} \text{ cm}^2/\text{Vsec} \qquad (1\text{-}4\text{-}1)$$

where ρ is the density of the material, E_1 is the "deformation potential" in eV per unit dilation, m_o and m_n^* are the free electron mass and effective mass of an electron in the conduction band, u is the sound velocity in the material.

(b) Polar Optical Phonon Scattering

At temperatures above 70K polar optical phonon scattering plays a very important role in the total scattering mechanism in n-InSb. The relative movement of the two different atom types causes a polarization of the crystal and a strong interaction with the carriers results. The mobility, limited by polar optical scattering only, is[16]

$$\mu_{op} = 1.7\times10^{30}\left(\frac{e}{e^*}\right)^2\left(\frac{m_o}{m_n^*}\right)^{-3/2} T^{\frac{1}{2}} Mv\,\frac{\omega_\ell}{2\pi}\,F\left(\frac{\theta_\ell}{T}\right)\left[\exp\left(\frac{\theta_\ell}{T}\right)-1\right] cm^2/Vsec. \quad (1\text{-}4\text{-}2)$$

Here e* is the effective charge[17], M is the reduced mass of the atoms, v is the volume of the unit cell, $\theta_\ell = \frac{\hbar\omega_\ell}{K_B}$ is the optical mode temperature and ω_ℓ is the longitudinal optical phonon frequency. $F(\frac{\theta_\ell}{T})$ has values between 0.6 and $0.375\ (\pi\theta_\ell/T)^{\frac{1}{2}}$.

Whenever holes have a much larger mass than electrons, the electron mobility may be reduced by electron-hole scattering. This process is important for intrinsic InSb and can be analyzed in the same way as ionized impurity scattering, discussed in the next section.

The effect of electron-electron scattering and screening of ions by carriers must be included in a total treatment of the mobility. For polar optical scattering, the interaction between the electrons and the lattice is reduced when there are large numbers of carriers present. Calculations by Ehrenreich[18] for InSb which include electron-

electron scattering and screening by carriers predict a $T^{-1.7}$ temperature dependence for combined polar optical and electron-hole scattering in the 100K-300K temperature region.

II. Low Temperature Case

(a) Ionized Impurity Scattering.

There may be large effects as a result of carriers scattered by ionized impurities. The mobility limit due to this scattering process is given by[19]

$$\mu_I = 3.2\text{x}10^{15}\left(\frac{m_o}{m_n^*}\right)^{\frac{1}{2}} \frac{\varepsilon^2 T^{3/2}}{N_{Di}+N_{Ai}} \Big/ \log\left[1.3\text{x}10^{14}T^2\varepsilon\left(\frac{m_n^*}{m_o}\right)\Big/n\right] \text{cm}^2/\text{Vsec.} \tag{1-4-3}$$

where N_{Di} and N_{Ai} are the concentrations of ionized donors and acceptors, n is the electron density in the conduction band and ε is the dielectric constant.

(b) Neutral Impurity Scattering.

Erginsoy[20] has given a simple treatment for the neutral impurity scattering process which is valid at low temperatures. The mobility limit due to this process is

$$\mu_N = 1.4\text{x}10^{22}\left(\frac{m_n^*}{m_o}\right) \frac{1}{\varepsilon N_N(T)} \text{ cm}^2/\text{Vsec.} \tag{1-4-4}$$

Here $N_N(T)$ is the concentration of neutral impurities and this may

increase considerably at low temperature due to carrier freeze-out. Since $m_n/m_o^* \approx 0.013$ in n-InSb at P = 0, neutral impurity scattering is relatively more important for this material when compared to other semiconductors with higher electron effective masses.

1-5. Hall Effect Measurements and the van der Pauw Technique

Van der Pauw[21] has developed a method of measuring the specific resistivity and Hall effect of flat samples of arbitrary shape. This method holds if the following conditions are fulfilled.

(a) The contacts are at the periphery of the sample.

(b) The contacts are sufficiently small.

(c) The sample is homogeneous in thickness.

(d) The surface of the sample is singly connected, i.e. the sample does not have isolated holes.

The expression for specific resistivity is given by

$$\rho = \frac{\pi d}{\ell n 2} \frac{(R_{AB,CD}+R_{BC,DA})}{2} f \left(\frac{R_{AB,CD}}{R_{BC,DA}}\right) \tag{1-5-1}$$

where d is the thickness of the sample, $R_{AB,CD}$ is the resistance defined as the potential difference between contacts D and C per unit current through contacts A and B. The resistance $R_{BC,DA}$ is defined similarly. The parameter f is a slowly varying function of the ratio $R_{AB,CD}/R_{BC,DA}$ and satisfies the relation

$$\frac{R_{AB,CD}-R_{BC,DA}}{R_{AB,CD}+R_{BC,DA}} = f \text{ arc cosh}\left\{\frac{\exp(\ln 2/f)}{2}\right\} \qquad (1\text{-}5\text{-}2)$$

The arrangement for specific resistivity measurement is shown in Fig. 2.

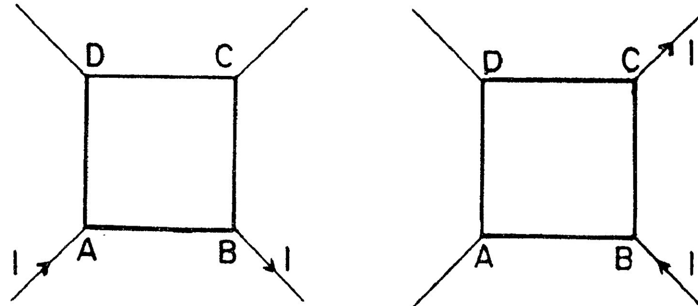

Fig. 2

The Hall coefficient R_H can be determined by measuring the change of the resistivity $\Delta R_{BD,CA}$ when a magnetic field $\vec{B}$ is applied perpendicular to the sample. Electron conduction processes dominate hole contributions in n type InSb for both the intrinsic and extrinsic regions. The ratio $\mu_n/\mu_p \simeq 100$ and in addition $n \gg p$ in the extrinsic temperature region. Because $\mu_n \gg \mu_p$ one may assume single band con-

duction for both the intrinsic and extrinsic limits in n-InSb, that is $\rho = (ne\mu_n)^{-1}$. The van der Pauw expression for the Hall coefficient is

$$R_H = \frac{d}{|\vec{B}|} \Delta R_{BD,CA} = \frac{\gamma_H}{ne} = \frac{1}{n_{eff}e} \qquad (1\text{-}5\text{-}3)$$

where $\gamma_H = \langle \mu_n{}^2 \rangle / \langle \mu_n \rangle^2$. The Hall factor γ_H varies from 1 to 2 depending on the scattering mechanism. While the contributions from the various scattering processes are not known too well, one may obtain the Hall mobility by leaving γ_H undetermined. Then since $\mu_H = \gamma_H \mu_D$ (μ_D = drift mobility)

$$\mu_H = \frac{R_H}{\rho} = \left(\frac{\gamma_H}{ne}\right) (ne\mu_{on}) = \gamma_H \mu_D \; . \quad \left(\mu_{on} = \mu_n(\vec{B}=0)\right) \qquad (1\text{-}5\text{-}4)$$

One must know γ_H in order to specify the drift mobility.

The apparent carrier concentration n_{eff} plotted as n throughout this thesis is obtained from

$$n_{eff} = \frac{|\vec{B}|}{de} \Delta R_{BD,CA} \; . \qquad (1\text{-}5\text{-}5)$$

For the purpose of obtaining pressure or temperature derivatives, there is negligible error introduced by plotting log n_{eff} instead of log n as their slopes are the same.

Fig. 3 shows the arrangement for Hall measurements.

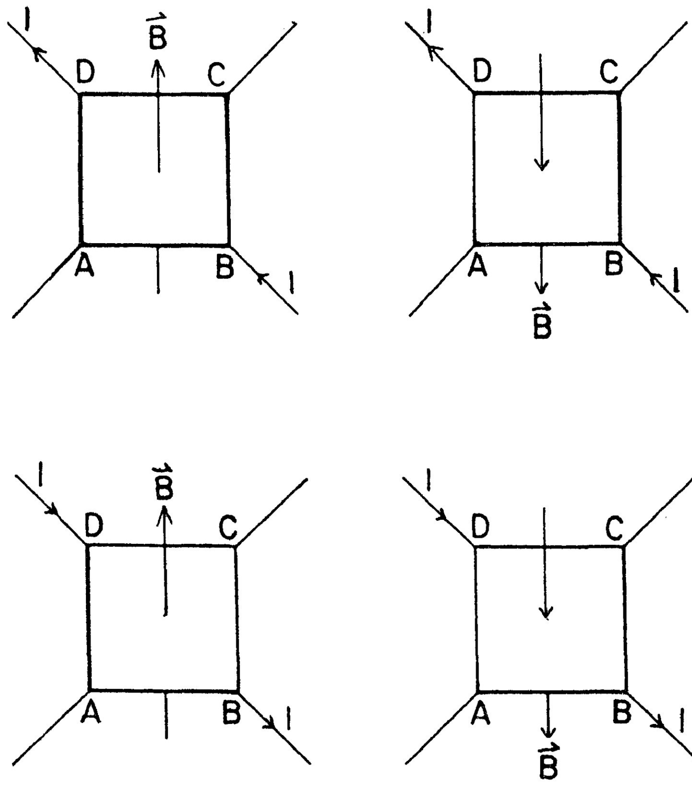

Fig. 3

Chapter 2

Equipment and Sample Preparation

2-1. The Pressure Vessel

A high pressure vessel with a self-stressing double walled cylinder capable of pressures to 30 kbars was used in the measurements. The piston and cylinder pressure vessel is shown in Fig. 4. All parts are of heat treated Beryllium-copper alloy 25 (unless otherwise indicated) which is one of the strongest, non-magnetic structural metals suited to studies involving magnetic fields. The Teflon capsule and the end plug are machined to be light push fits to the inner bore.

2-2. Sample Preparation

The specimens used in the measurement were approximately 0.5x1.5x1.5 mm and were cut from a single crystal ingot in n-InSb. The ingot was mounted on a carbon cutting palette using black sealing wax. A wire saw employing an endless loop of wire and an oil slurry was used in cutting the sample. The slurry consisted of 600 grit SiC and Buehler Automet lapping oil which is water soluble. After cutting, the sample was rinsed with trichloroethylene and then etched for about 2 to 3 seconds in CP4A etchant which was prepared by mixing 15 ml of HF, 25 ml of HNO_3 and 25 ml of CH_3COOH. The sample was then rinsed again in methanol and trichloroethylene and air dried.

Figure 4. High-pressure vessel with self-stressing, double walled cylinder. The Teflon capsule is filled with a 1:1 mixture of isoamyl alcohol and n-pantane. All other parts are of hardened Be-Cu, except for the tungsten-carbide piston (WC piston) and the ½ hard Be-Cu capsule plug and cap.

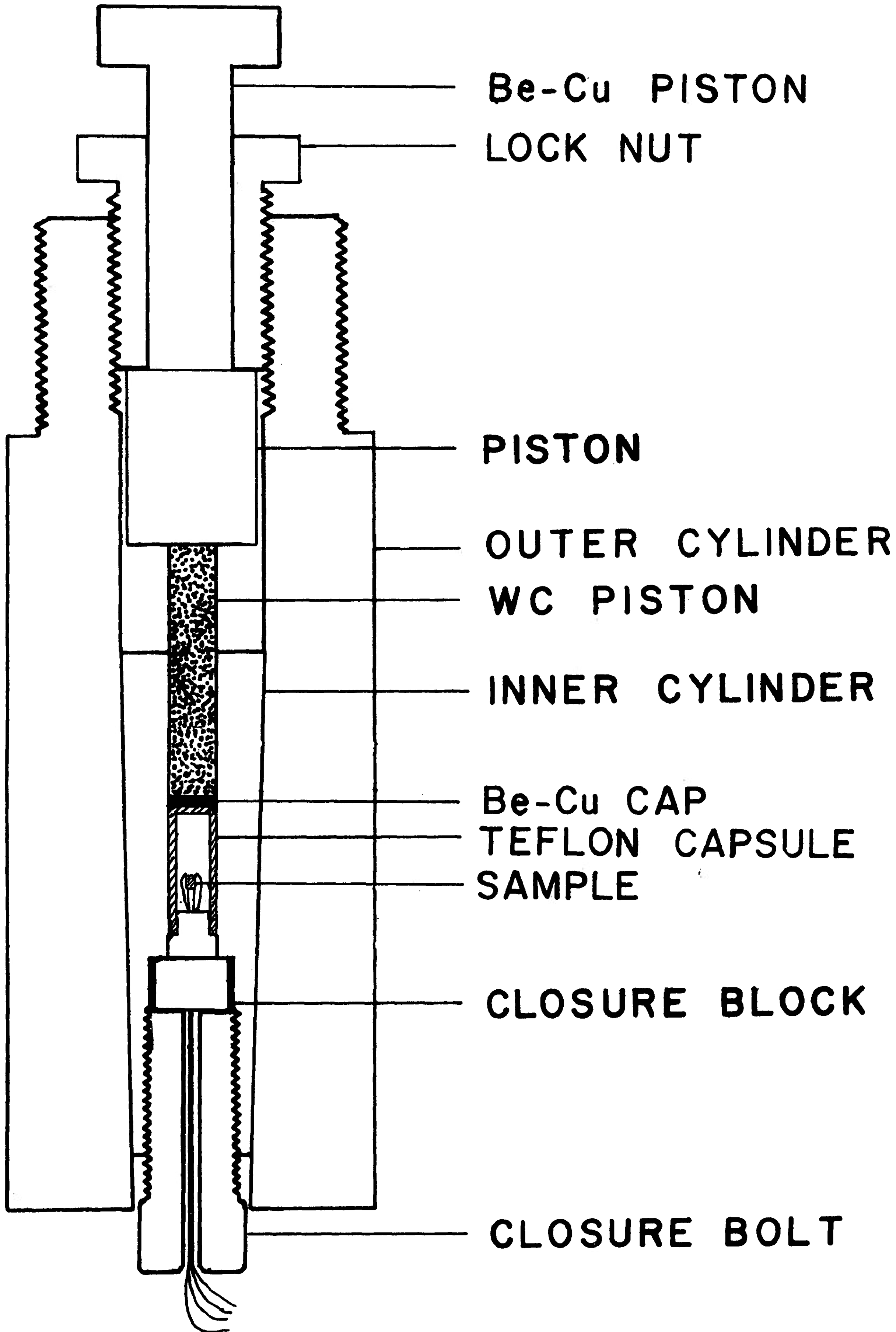
Be-Cu PISTON
LOCK NUT
PISTON
OUTER CYLINDER
WC PISTON
INNER CYLINDER
Be-Cu CAP
TEFLON CAPSULE
SAMPLE
CLOSURE BLOCK
CLOSURE BOLT

The electrical connections were made by soldering 0.003 inch platinum wires to the sample with Indium solder containing 2% tellurium. The tellurium reduces the possibility of forming a p-n junction at the contact. Platinum wires were then connected to the copper feed through wires. This was required because copper has a high diffusion coefficient for most semiconductors including InSb, and a direct connection would lead to sample contamination by the copper.

The sample was then encapsulated in a teflon capsule filled with a 1:1 mixture of isoamyl alcohol and n-pentane which acted as a pressure transmitting fluid. The encapsulated sample was then inserted into the bore of the inner cylinder and sealed with the closure bolt. After assembly the inner cylinder was pressed into the outer cylinder by a 2×10^4 N thrust. This reduces the inner bore diameter slightly and provides the necessary initial seal which prevents the pressure fluid from leaking through the common surfaces between the teflon capsule and the end plug. The pressure vessel was then mounted in a press frame and the sample was pressurized by applying a force to the upper Be-Cu piston. The pressure could be locked in by use of the nut which is coaxial with the thrust piston.

2-3. Experimental Methods

One of the problems of pressure measurements carried out over a large temperature range is differential contraction pressure loss.

The contraction rate for the metal in the pressure vessel is usually less than that of the pressure fluid and this leads to a loss in pressure during cool-down. In order to try to obtain estimates of pressure loss during cool-down we first performed a series of constant temperature variable pressure measurements for ρ and R_H at 296K, 198K (dry ice in acetone) and 77K. This proved possible at 198K and 77K because the pressure vessel could be pressurized in stages after first pre-cooling. There appeared to be about a 15% loss in pressure at 198K and a 25% loss at 77K when first pressurized at 296K.

When making temperature measurements on the helium refrigerator we pressurized at room temperature initially and then estimated the low temperature pressure from the resistivity at 77K. Below 77K where thermal expansions are small, we assumed the differential contraction pressure loss was negligible.

The van der Pauw method was employed in the Hall measurements. A Hewlett Packard model 419A Null DC voltmeter was used to measure the potential drop across the sample and the potential across a standard resistor in series with the sample. All thermomagnetic effects except the Ettingshausen effect were eliminated from the Hall voltage readings by reversing the current and magnetic field directions and taking the appropriate averages. The Ettingshausen effect has the same current and field dependence as the Hall effect and so cannot be eliminated in this way. But this effect is small and requires a temperature gradient, and since we controlled temperature for 10 to

30 minutes at each setting before taking the readings, this effect was negligible. Changes in the sample dimensions with pressure were not taken into account since this is only 3% in volume or 1% in length at 15 kbar in InSb. The sample thickness d appears in the van der Pauw equation, therefore this changes by about 1% at 15 kbar.

Chapter 3

Results and Discussions

3-1. Constant Temperature Variable Pressure Results

Detailed measurements of electrical resistivity $\rho(P)$ and carrier concentration $n(P)$ as a function of pressure at constant temperature were made over the pressure range from 0 to 15 kbar. Hall mobility was calculated from the resistivity and carrier concentration data by using equations (1-5-1), (1-5-4) and (1-5-5). Fig. 5a, 5b, Fig. 6a, 6b and Fig. 7 show the pressure dependence of $\rho(p)$, $n(P)$ and $\mu(P)$ for T = 296K, 198K and 77K, respectively.

When the large increase in resistivity was first seen at 77K it was felt that the sample had broken, but further investigation showed that the resistivity was changing reproducibly. In fact, the large resistance increase is due to a large reduction in the carrier concentration as shown in Fig. 6b, since $\rho = \frac{1}{ne\mu}$.

3-2. Constant Pressure Variable Temperature Results

A systematic investigation of the "transition" was carried out by reducing pressure and taking Hall and resistivity data from 296K to 6.4K.

The Hall mobility $\mu(T)$ was obtained by measuring $\rho(T)$ and $n(T)$ by the van der Pauw method and using equation (1-5-4).

Fig. 8 shows the temperature dependence of Hall mobility for different pressures. The regions where $\mu(T)$ decreases below the

Figure 5a. Resistivity vs pressure for n-InSb at T = 296K. The hysteresis loop may be used to calibrate the pressure.

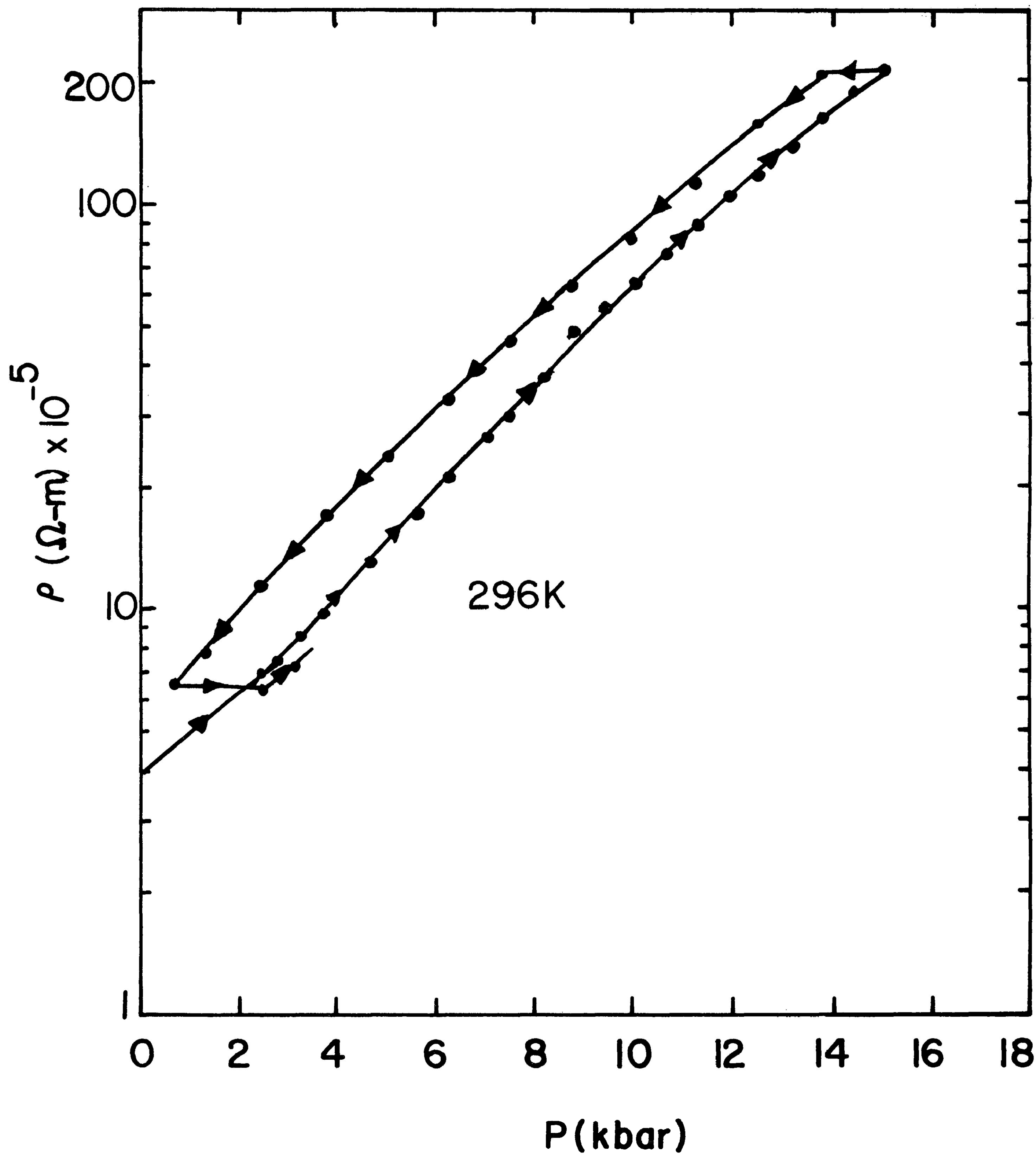

200
100
10
1
ρ (Ω-m) x 10^-5
296K
0
2
4
6
8
10
12
14
16
18
P (kbar)

Figure 5b. Resistivity vs pressure for n-InSb at T = 198K and 77K.

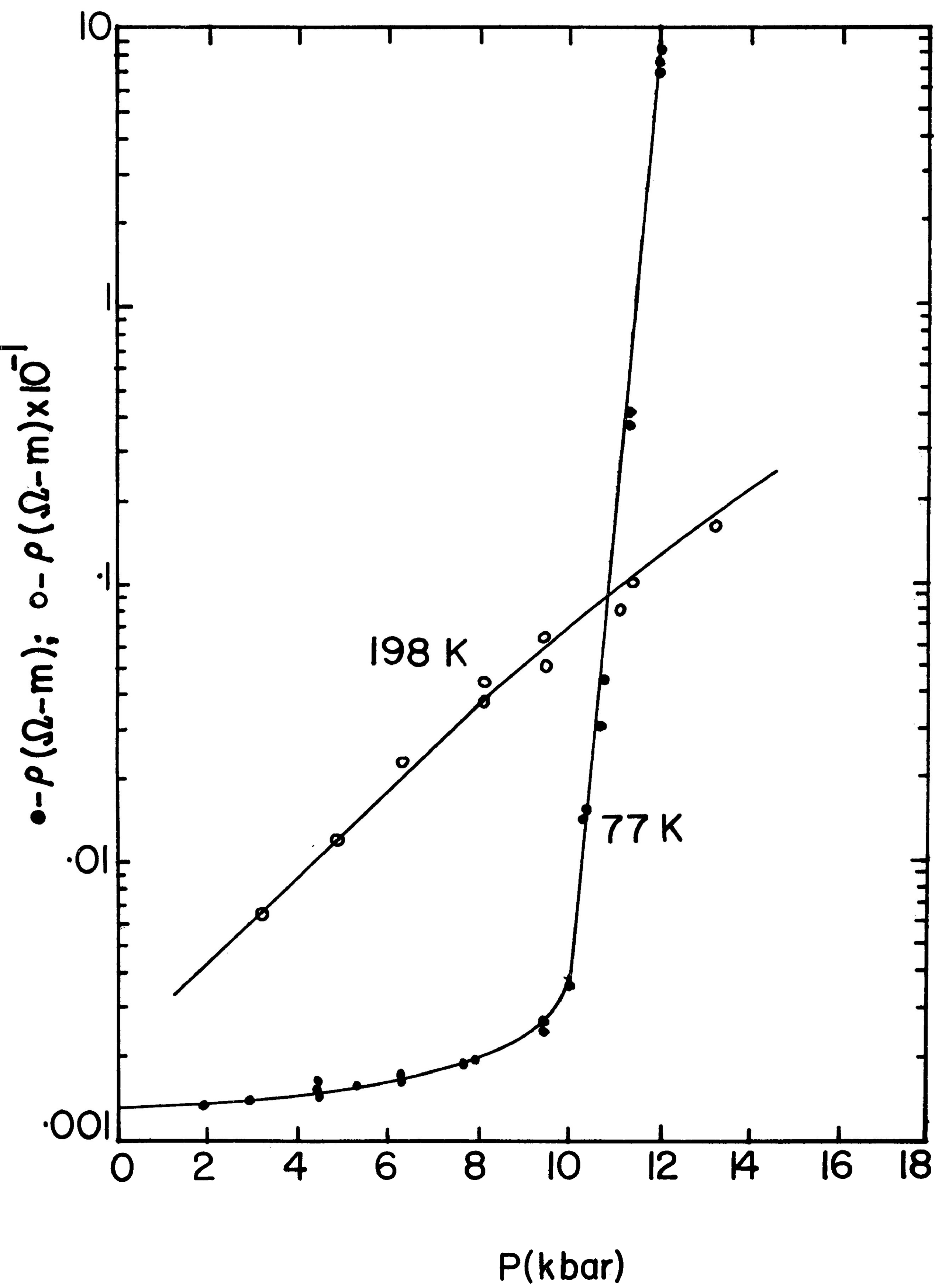

10
1
·1
·01
·001
0
2
4
6
8
10
12
14
16
18
198 K
77 K
P(kbar)
●- ρ (Ω-m); ○- ρ (Ω-m) x 10⁻¹

Figure 6a. Carrier concentration n vs pressure P for n-InSb at T = 296K.

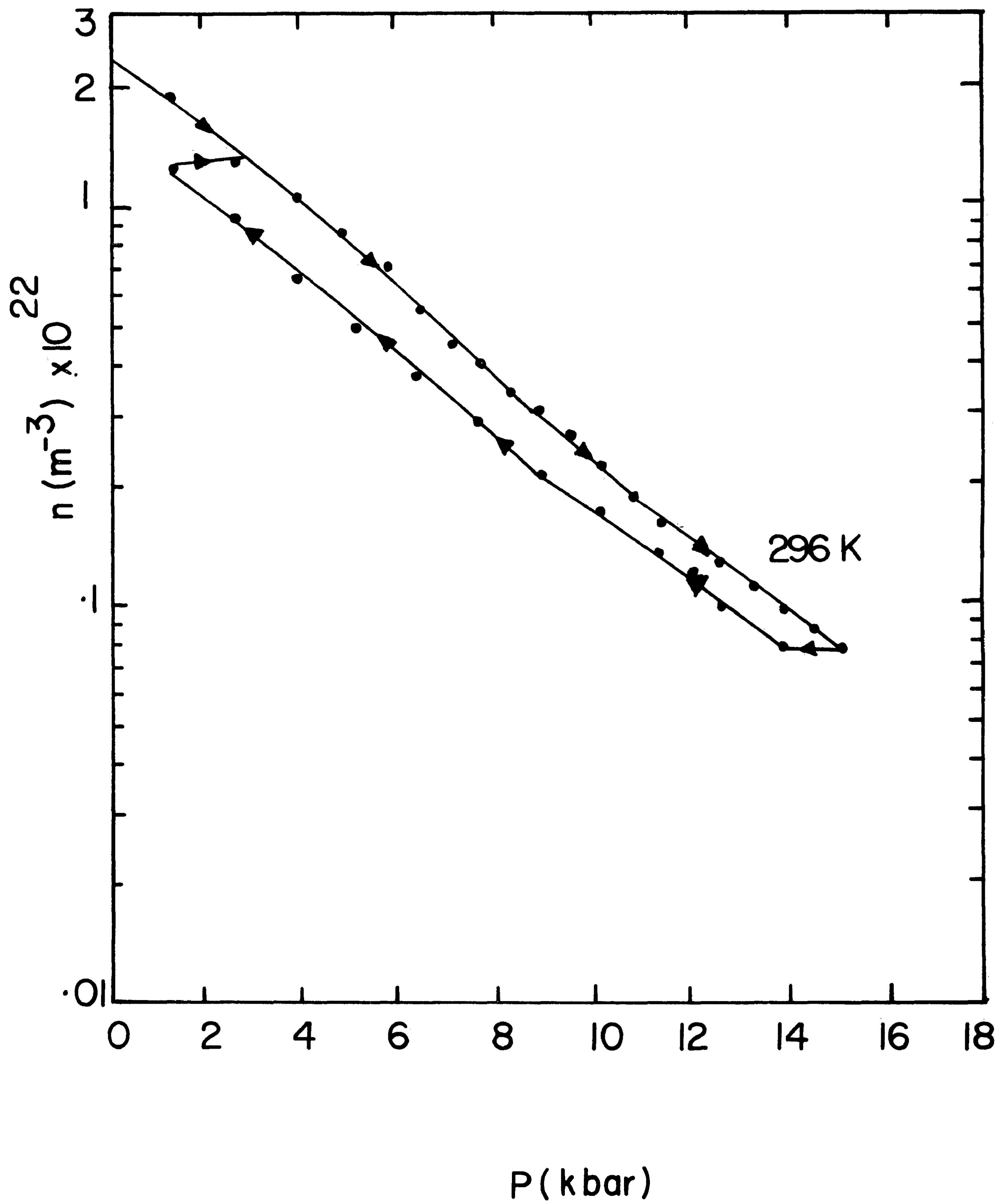

3
2
1
·1
·01
0
2
4
6
8
10
12
14
16
18
n (m⁻³) x 10²²
296 K
P (k bar)

Figure 6b. Carrier concentration n vs pressure P for n-InSb at T = 198K and 77K.

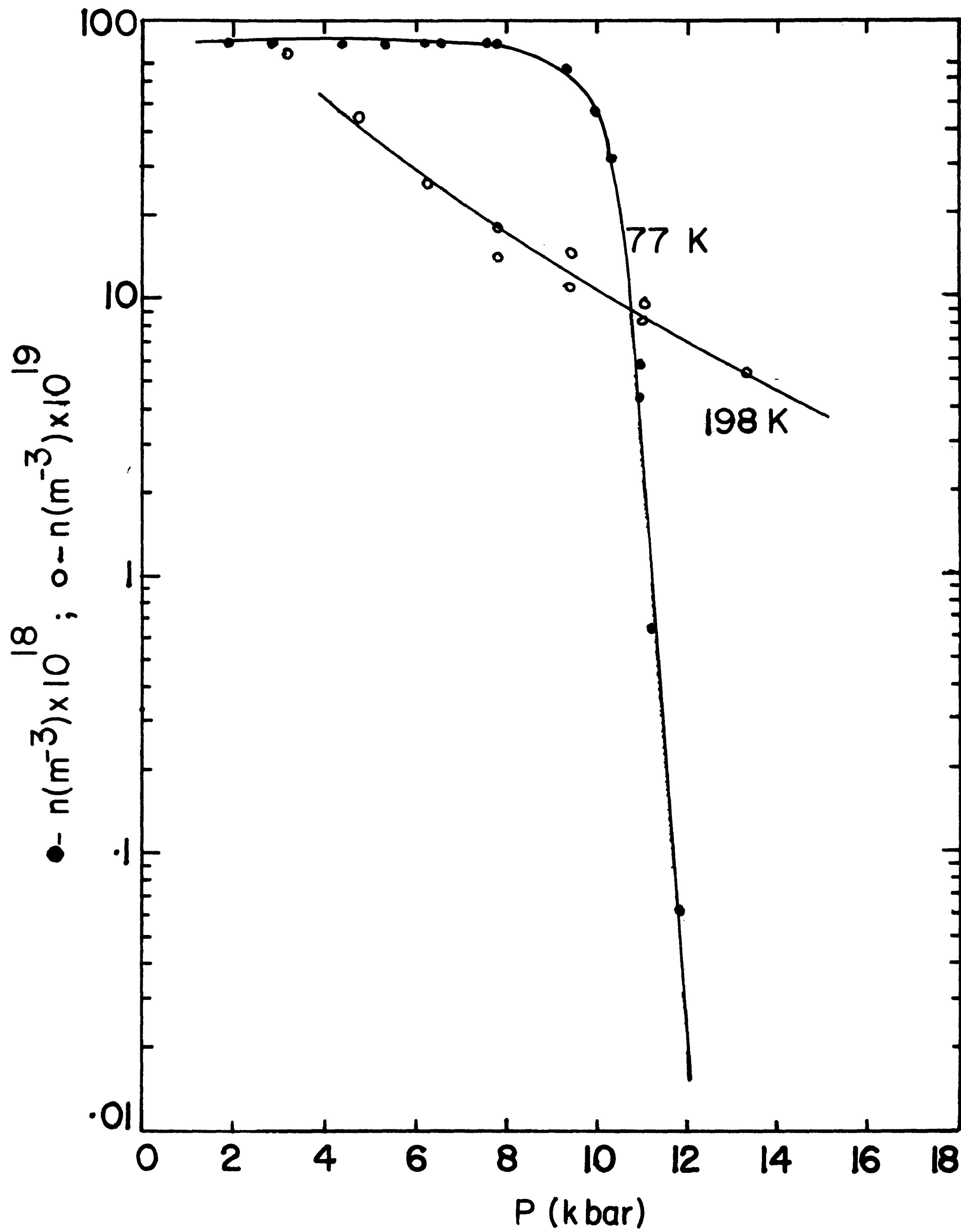

100
10
1
·1
·01
77 K
198 K
●– n(m⁻³)x10^18 ; o– n(m⁻³)x10^19
0
2
4
6
8
10
12
14
16
18
P (k bar)

Figure 7. Hall mobility μ vs pressure P for n-InSb at T = 296K, 198K and 77K.

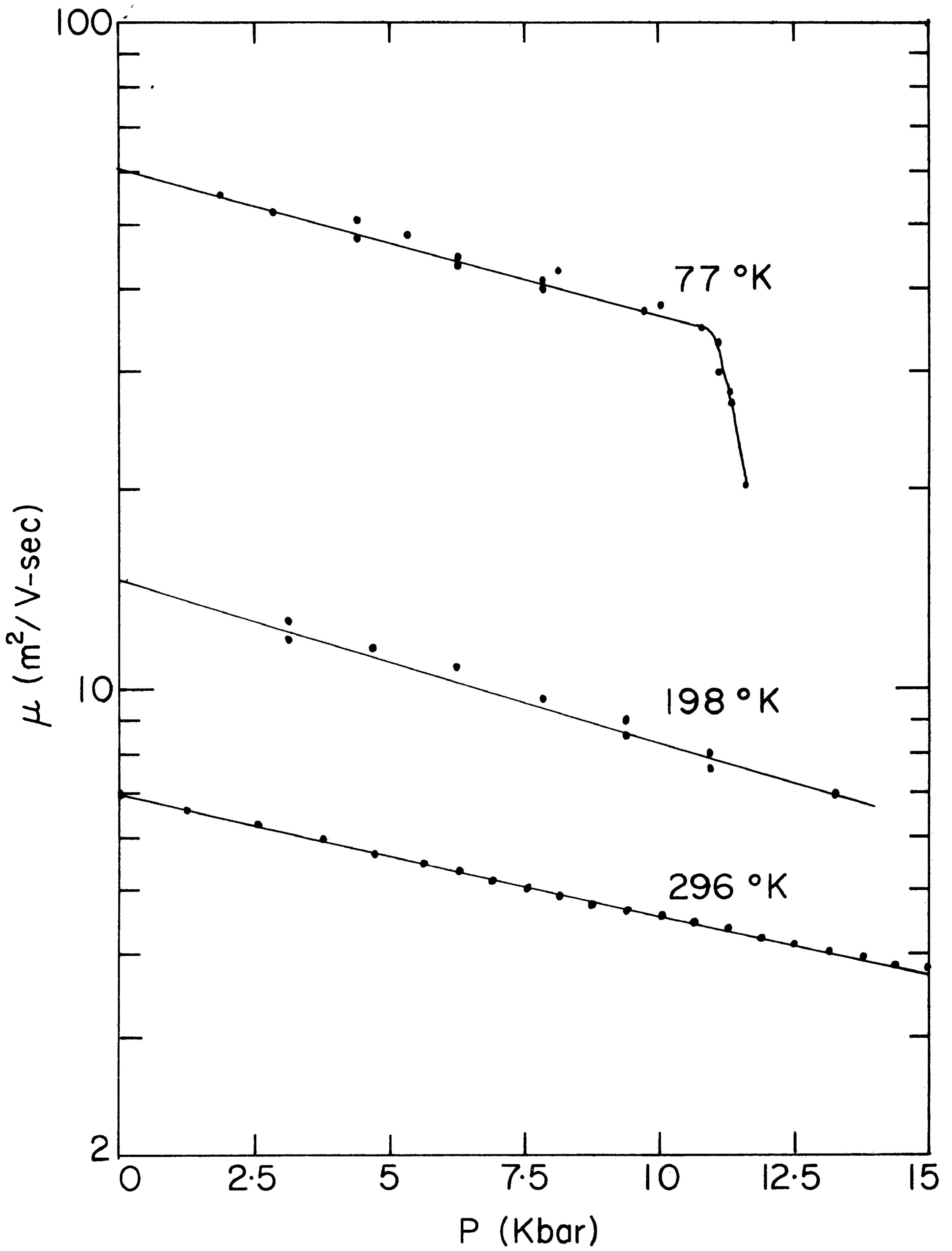
100
10
2
0
2·5
5
7·5
10
12·5
15
P (Kbar)
μ (m²/ V-sec)
77 °K
198 °K
296 °K

general curve indicate where carrier freeze-out has almost become complete and $n \ll N_D$. A plot of $\rho(T)$ vs T for different pressures is shown in Fig. 9. The donor gap increases strongly with increasing pressure and this shows up in $\rho(T)$ at low temperature. The pressure dependence of the donor gap is discussed in section 3-4.

3-3. Temperature and Pressure Dependence of the Hall Mobility

(a) Temperature dependence

Fig. 8 shows the Hall mobility as a function of temperature for different pressures. The best fit to the zero pressure mobility from 80K-300K occurred for a $T^{-(1.75\pm0.05)}$ law, which is in very good agreement with Ehrenreich's $T^{-1.7}$ prediction. Increasing pressure resulted in a general shift to lower absolute mobilities with the same apparent temperature dependence.

In attempting to fit to the low temperature (6K-50K) Hall mobility curve we substituted measured values of n and T into equations (1-4-3) and (1-4-4) for μ_I and μ_N. In the expression for μ_I we set $n = N_{Di} + N_{Ai}$ which is equivalent to setting $N_{Ai} \simeq 0$. Again we set $m_n^*/m_o = 0.013$ and $\varepsilon = 18$. Because m_n^*/m_o is so small for electrons in InSb and because the ratio μ_N/μ_I is proportional to $(m_n^*/m_o)^2$, the low temperature mobility $\frac{1}{\mu_C} = \frac{1}{\mu_N} + \frac{1}{\mu_I}$ is essentially determined by neutral impurity scattering with μ_N^{-1}/μ_I^{-1} remaining close to 6 from 6.3K to 40K. For neutral impurity concentration we chose

Figure 8. Hall mobility μ vs temperature T for n-InSb at different pressures.

△ P = 0 kbar

• P = 4.2 kbar

□ P = 8.2 kbar

▲ P = 10.3 kbar

○ P = 12.4 kbar

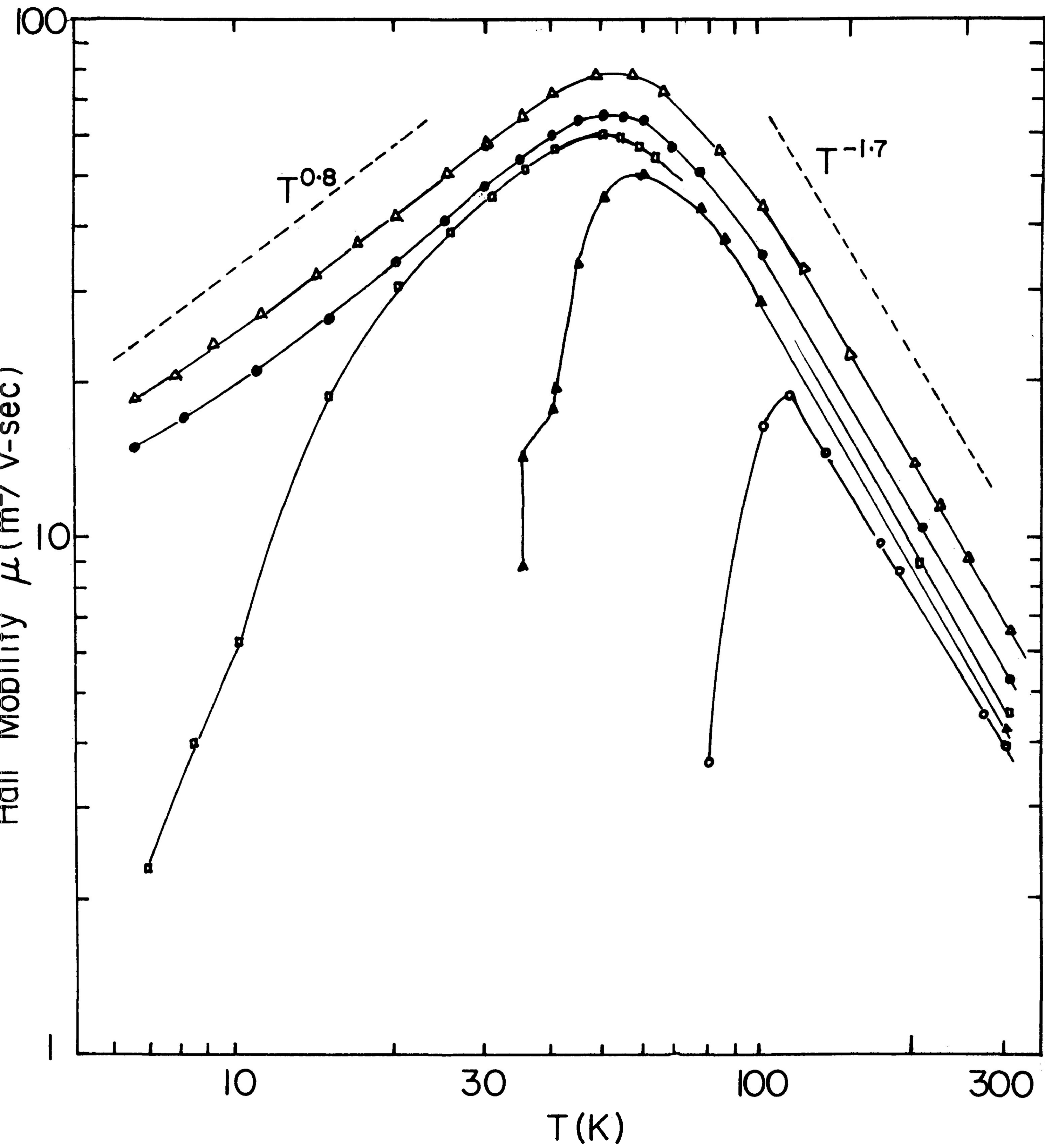

100
10
1
Hall Mobility μ (m²/ V-sec)
$T^{0.8}$
$T^{-1.7}$
10
30
100
300
T (K)

Figure 9. Resistivity ρ vs temperature T for n-InSb at different pressures.

- ⚲ P = 0 kbar
- ⊙ P = 4.2 kbar
- ▲ P = 8.2 kbar
- ⧖ P = 9.7 kbar
- ● P = 10.3 kbar
- ○ P = 12.4 kbar

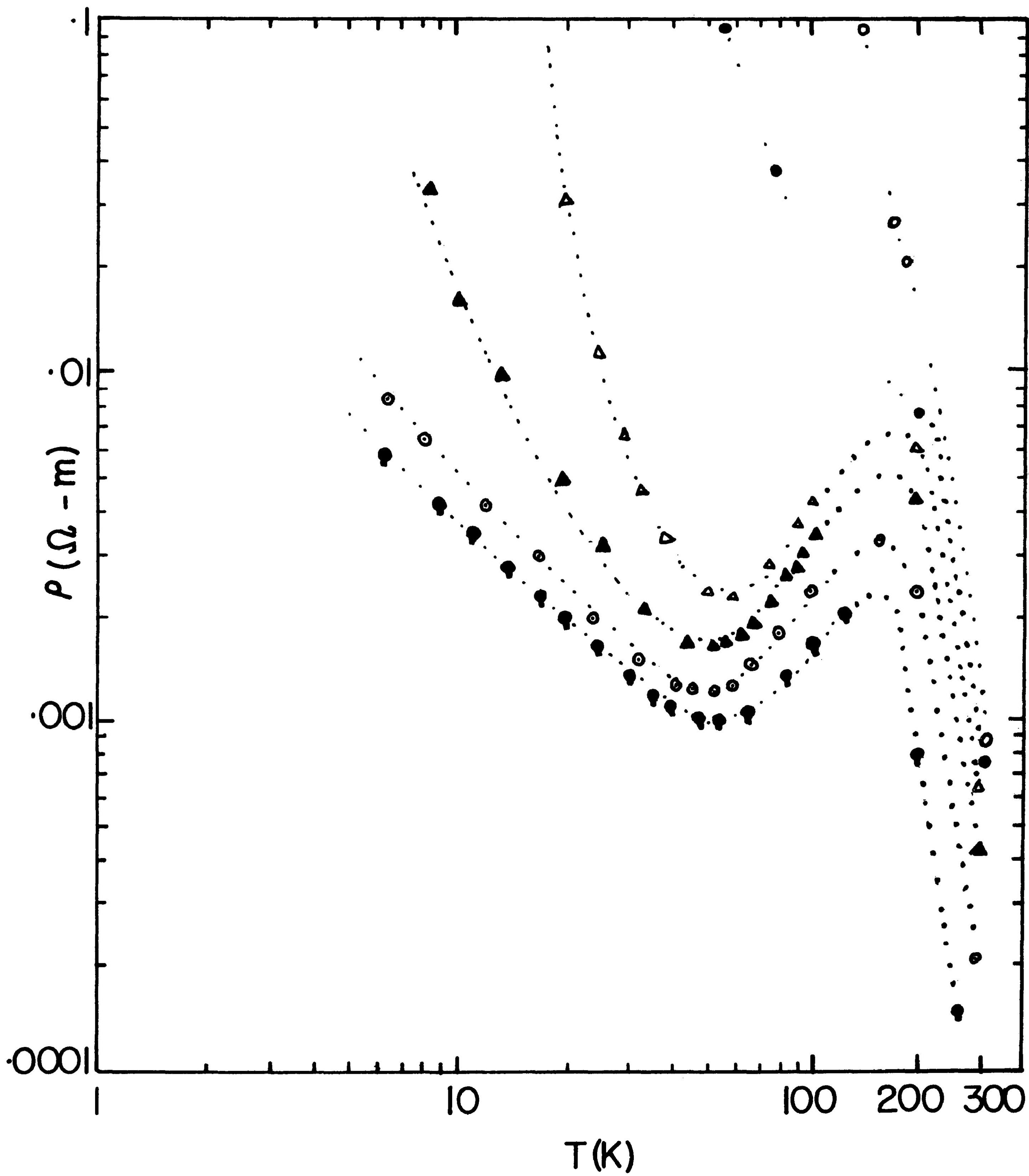

·1
·01
·001
·0001
ρ (Ω - m)
1
10
100
200
300
T(K)

$N_N(T) = n(77K) - n(T)$. The absolute mobility calculated in this way was approximately 1.8 times larger than the measured mobility although the temperature dependence was correct. One could achieve very close fit by simply reducing the coefficients by this factor. The $T^{0.8}$-dependence is due to the temperature dependence in the neutral impurity concentration, N_N, as well as the temperature dependence of $T^{3/2}/n(T)$ in the ionized impurity mobility term. Both of these are close to a $T^{0.8}$ dependence. The importance of μ_N instead of μ_I in determining the magnitude of μ_C is largely due to the small effective mass ratio (m_n^*/m_o) and the way it appears in the two expressions.

(b) Pressure Dependence of the Hall Mobility (77K-300K)

Fig. 7 shows the pressure dependence of the Hall mobility for 296K, 198K and 77K, while Fig. 10 shows the same data plotted against the energy gap E_g on a log-log plot. Using the fact that $E_g \alpha m_n^*$, one may determine the power of r in $\mu \alpha m_n^* \alpha E_g{}^r$ through

$$d\ell n\mu/d\ell n E_g = r .$$

As seen from the agreement with a $T^{-1.7}$ temperature dependence, the mobility is limited by a combination of polar optical and electron-hole scattering in the 80K to 300K range. Also one expects an increase in the relative importance of the electron-hole (ionized impurity like) scattering term as temperature increases and the number of electron-hole pairs increase.

Figure 10. A plot of mobility μ vs intrinsic gap E_g for n-InSb at T = 296K, 198K and 77K.

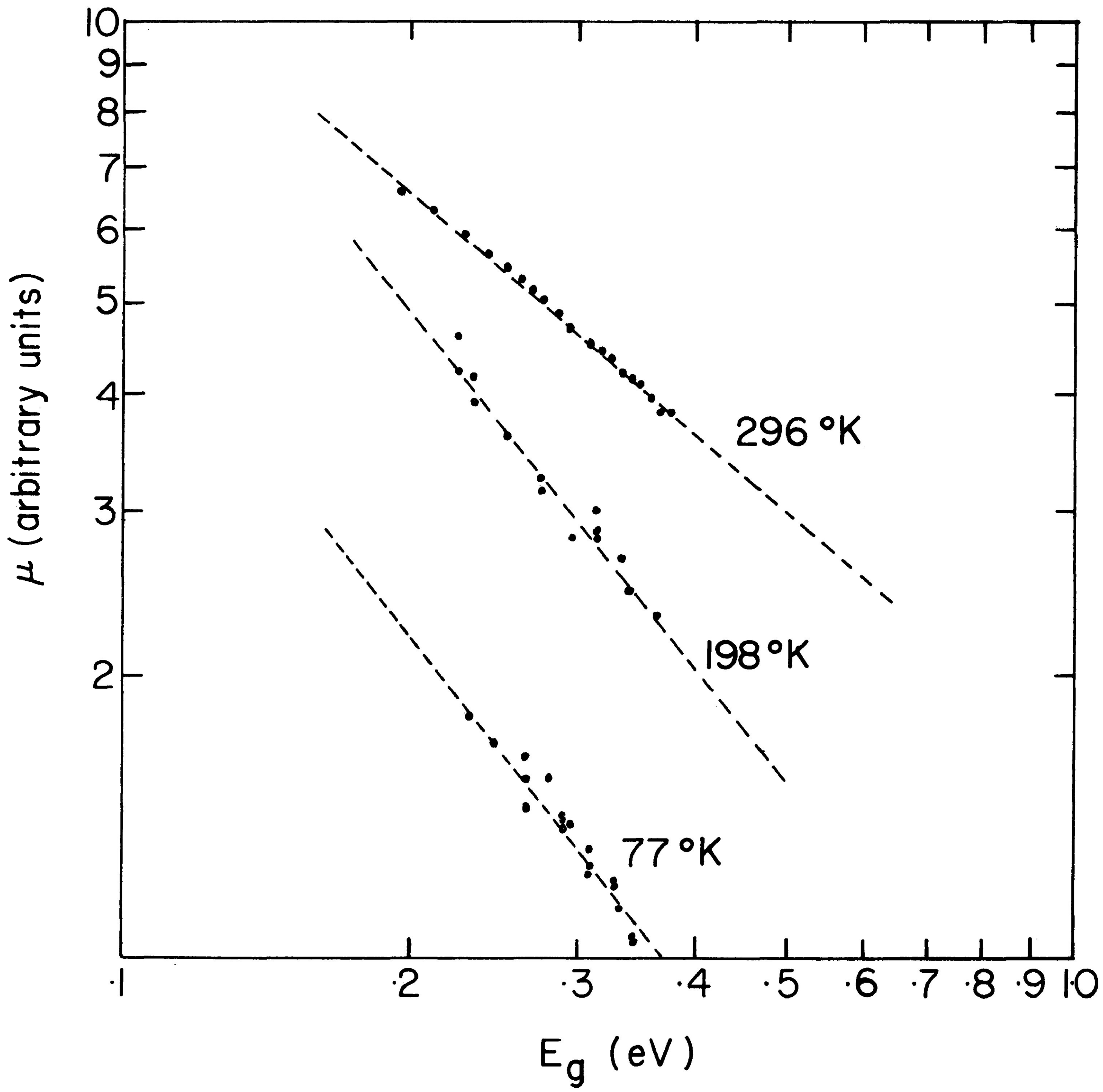

10
9
8
7
6
5
4
3
2
μ (arbitrary units)
296 °K
198 °K
77 °K
·1
·2
·3
·4
·5
·6
·7
·8
·9
1·0
Eg (eV)

Assuming that electron-hole scattering is negligible at 77K so that only polar optical scattering is important, from equation (1-4-2) we may set

$$\frac{d\ell n\mu_{op}}{d\ell nE_g} = \frac{d\ell n\mu_{op}}{dP}\bigg/\frac{d\ell nE_g}{dP}$$

Tetrahedrally bonded semiconductors have a small Grüneisen γ and a value of about -1.2 for germanium[22] at longitudinal optical frequencies should also be a reasonable estimate for InSb. That is, $d\log\theta_\ell/d\log v \simeq -1.2$, where v is the volume.

Assuming a compressibility of about 2.2×10^{-6} bar^{-1} for InSb (since III-V compounds have compressibilities similar to those of the group IV semiconductors) a pressure of 15 kbar decreases the specific volume by 3% and hence increases θ_ℓ by about 3.6%. Since $\theta_\ell \approx 260$K at P = 0, it increases to $\theta_\ell \approx 268$K at 15 kbar. $F(\theta_\ell/T)$ is a slowly varying function of T and P, so we ignore its pressure derivative. Cancelling the increase in ω_ℓ with the decrease in v we have at 77K

$$\frac{d\ell n\mu_{op}}{dP} = -\,1.5\,\frac{d\ell nm_n^*}{dP} + \frac{d\ell n}{dP}\left[\exp\left(\frac{\theta_\ell}{T}\right) - 1\right]$$

But $\frac{d\ell nm_n^*}{dP} = \frac{d\ell nE_g}{dP} = .052$ kbar^{-1} (ignoring uncertainty for this calculation) so

$$\frac{d\ell n\mu_{op}}{d\ell nE_g} = -1.5 + \frac{1}{0.052}\ \frac{\delta\ell n}{\delta p}\left[\exp(\theta_\ell/T)\ -1\right] = -1.36 = r_{op}$$

at 77K assuming no electron-hole scattering. This is in good agreement with the measured value of - 1.30 ± 0.1 at 77K.

At 296K, $d\ell n\mu_{op}/d\ell nE_g \simeq -1.43$ using the same pressure assumptions. Here, however, the number of charged scattering centers (ionized donors plus heavy holes) has increased by about 185 times at P = 0 and 15 times at P = 15 kbar since they must equal n. Therefore, as a function of increasing pressure at 296K, the mobility derivative $\frac{d\ell n\mu}{d\ell nE_g}$ may contain a sizeable ionized impurity contribution.

We first estimate $d\ell n\mu_I/d\ell nE_g = r_I$. From equation (1-4-3) we may set

$$\frac{d\ell n\mu_I}{dP} = -\frac{1}{2}\frac{d\ell nm^*_n}{dP} - \frac{d\ell nn}{dP} - \frac{d\ell n}{dP}\left\{\log\left[1.3\text{x}10^{14}\ \frac{T^2\varepsilon}{n}\ \left(\frac{m^*_n}{m_o}\right)\right]\right\}\ .$$

Using $\varepsilon = 18$, measured values of n and the fact that $d\ell nm^*_n/dP = d\ell nE_g/dP = 0.052\ \text{kbar}^{-1}$, gives

$$r_I = d\ell n\mu_I/d\ell nE_g \approx 2.642 \quad \text{at 296K.}$$

Similarly, at 77K where $d\ell nn/dP \simeq 0$, $d\ell n\mu_I/d\ell nE_g = -0.51 = r_I$.

To estimate the contribution of μ_I to the measured mobility μ_m at 296K we now estimate μ_I from equation (1-4-3). At T = 296K, $\mu_I \simeq 59.6$ m /Vsec, and any carrier screening effect is accounted for by the denominator. It is harder to obtain an absolute estimate of μ_{op} because screening has not been included explicitly in equation (1-4-2). Therefore, we attribute the remainder of the scattering to polar optical phonons and from

$$\frac{1}{\mu_m} = \frac{1}{\mu_{op}} + \frac{1}{\mu_I} \quad ; \quad \mu_I{}^{-1}/\mu_m{}^{-1} \simeq 0.124.$$

It can be shown that a combined r_c is simply the sum

$$r_c = r_{op}(\mu_{op}{}^{-1}/\mu_m{}^{-1}) + r_I(\mu_I{}^{-1}/\mu_m{}^{-1}) \ .$$

Table 1 lists the results for 77K, 198K and 296K.

The excellent agreement is probably somewhat fortuitous since we calculate μ_I and leave the remainder of the mobility to a screened μ_{op}. Nevertheless, the result supports the suggested increasing importance of electron-hole scattering at room temperature. It is gratifying to see that <u>both</u> the pressure and temperature dependence of μ_H are in agreement with Ehrenreich's prediction.

TABLE 1

T	$r_{measured}$	r_{op}	r_I	r_c	μ_I^{-1}/μ_m^{-1}
77K	-1.30±0.1	-1.36	-0.51	-1.34	0.026
198K	-1.28±0.1	-1.43	+2.45	-1.24	0.050
296K	-0.85±0.05	-1.44	+2.642	-0.91	0.124

3-4. Pressure Dependence of the Donor Gap E_D

The material studied was "pure" undoped n-InSb as evidenced by the high maximum mobility of approximately $8\times10^5\, cm^2/Vsec$ at 50K and zero pressure. Therefore, the equation discussed in section 1-3 is applicable to our present case. Rewriting it

$$\frac{n^2}{N_D-n} = \frac{N_c}{g_D} \exp\left(-\frac{E_D}{K_B T}\right),$$

where $N_c = 2(2\pi m_n^* K_B T/h)^{3/2}$ for a parabolic conduction band limit. A semilog plot of $\frac{n^2 T^{-3/2}}{N_D-n}$ vs $\frac{1}{T}$ is shown in Fig. 11a, 11b which appears to be temperature independent because it has a constant slope. These curves clearly indicate that for the extreme extrinsic region under study the carrier number is less than the number of donors and that carrier freeze-out or de-ionization across a donor energy gap E_D is

Figure 11a. A semilog plot of $n^2/(N_D - n)T^{3/2}$ vs $\frac{1}{T}$ for n-InSb at pressures P = 4.4 kbar, 8.1 kbar and 9.7 kbar. N_D is the number of donors per unit volume.

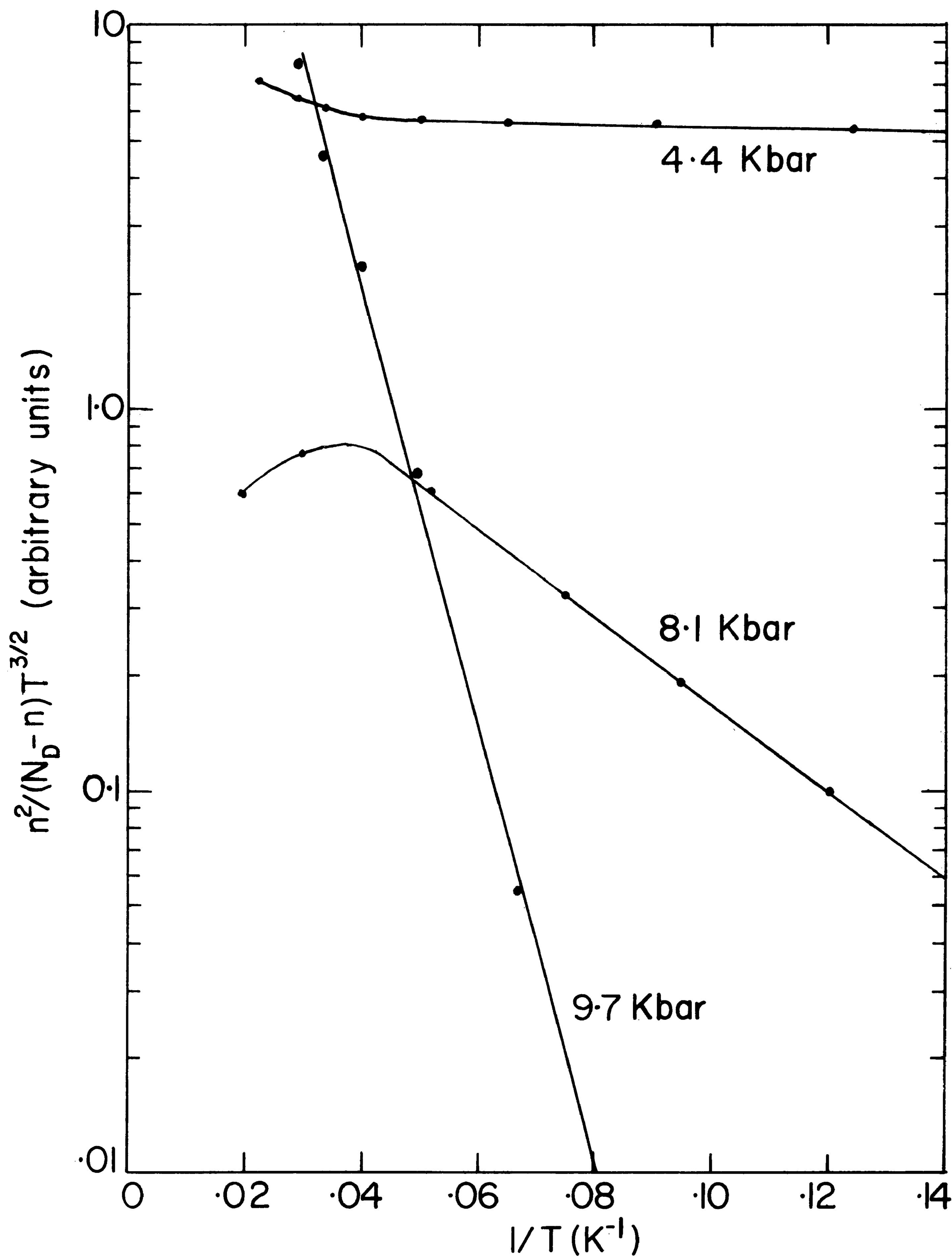

10
1·0
0·1
·01
0
·02
·04
·06
·08
·10
·12
·14
1/T (K⁻¹)
n²/(N_D−n)T^{3/2} (arbitrary units)
4·4 Kbar
8·1 Kbar
9·7 Kbar

Figure 11b. A semilog plot of $n^2/(N_D - n)T^{3/2}$ vs $\frac{1}{T}$ for n-InSb at pressures P = 11 kbar and 12.6 kbar. The upper side scale is for the 11 kbar curve.

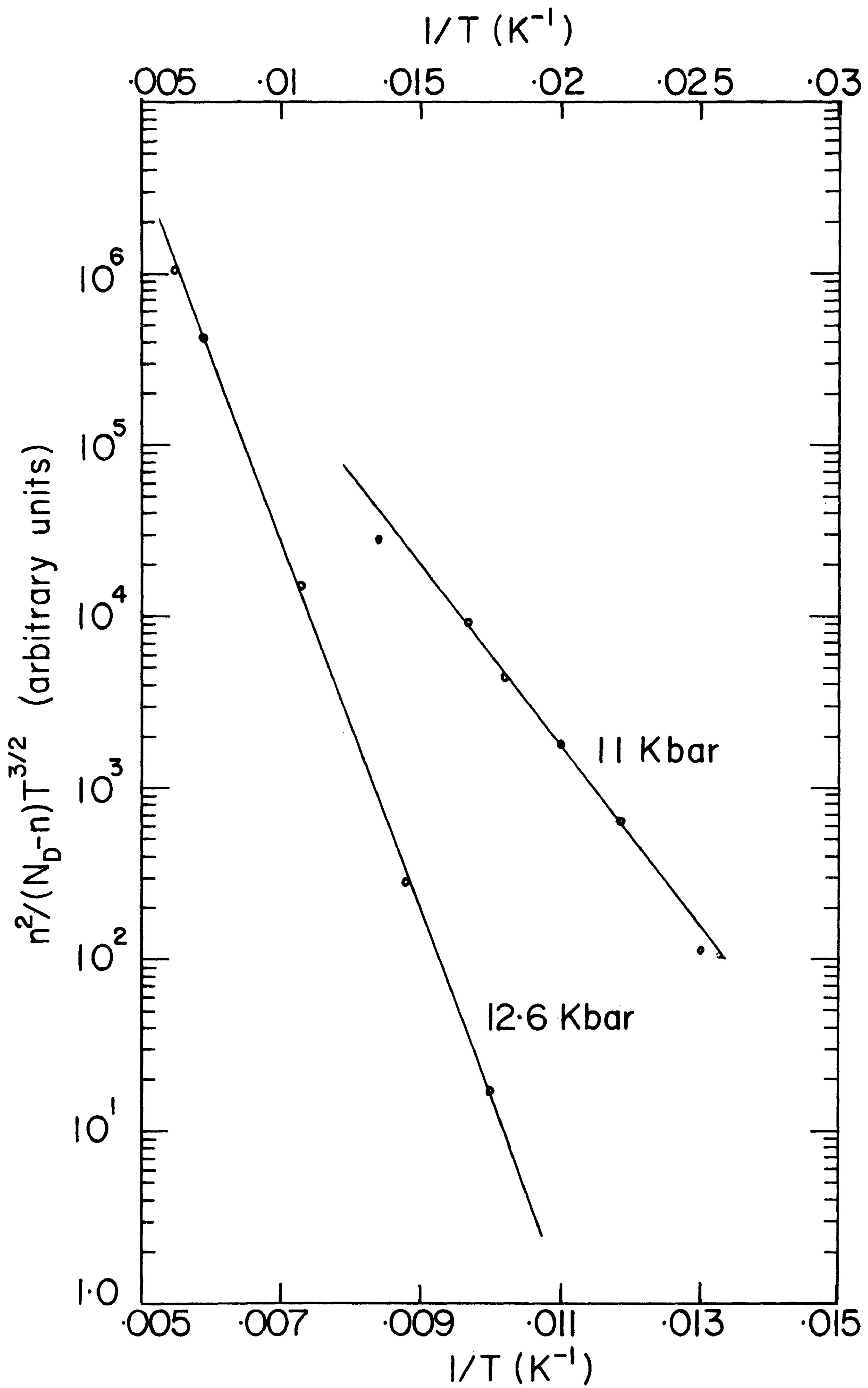
1/T (K⁻¹)
·005
·01
·015
·02
·025
·03
$n^2/(N_D-n)T^{3/2}$ (arbitrary units)
10^6
10^5
10^4
10^3
10^2
10^1
1·0
11 Kbar
12·6 Kbar
·005
·007
·009
·011
·013
·015
1/T (K⁻¹)

responsible for the decrease of n with decreasing temperature and/or increasing pressure.

From equation (1-3-4) one can obtain the expression

$$\frac{d\ell n\left[\frac{n^2}{(N_D-n)T^{3/2}}\right]}{d(\frac{1}{T})} = -\frac{E_D}{K_B} .$$

Fig. 12 shows the values of $E_D(P)$ obtained for several pressures. Since the donor gap varies approximately exponentially with pressure, this shows up as an apparent transition in ρ vs P data. Since

$$n \simeq n_o \exp\left(-\frac{E_D}{2K_BT}\right) \quad \text{and } \rho \propto n^{-1},$$

an exponential increase in E_D with increasing pressure produces an exponential of an exponential in ρ.

The rapid increase in E_D with pressure is still not completely understood. While Sladek[1] and other workers have seen magnetic freeze-out in n-InSb experimentally and many theoretical calculations have been carried out for this effect, no systematic pressure study on E_D in undoped n-InSb has been reported to our knowledge.

In the magnetic case of P = 0 and low temperature[23], the shallow impurity levels overlap the conduction band for zero magnetic field. Application of a magnetic field shifts the atomic

Figure 12. A semilog· plot of donor gap E_D vs pressure P

⊡ indicates the value obtained by S. Porowski.[11]

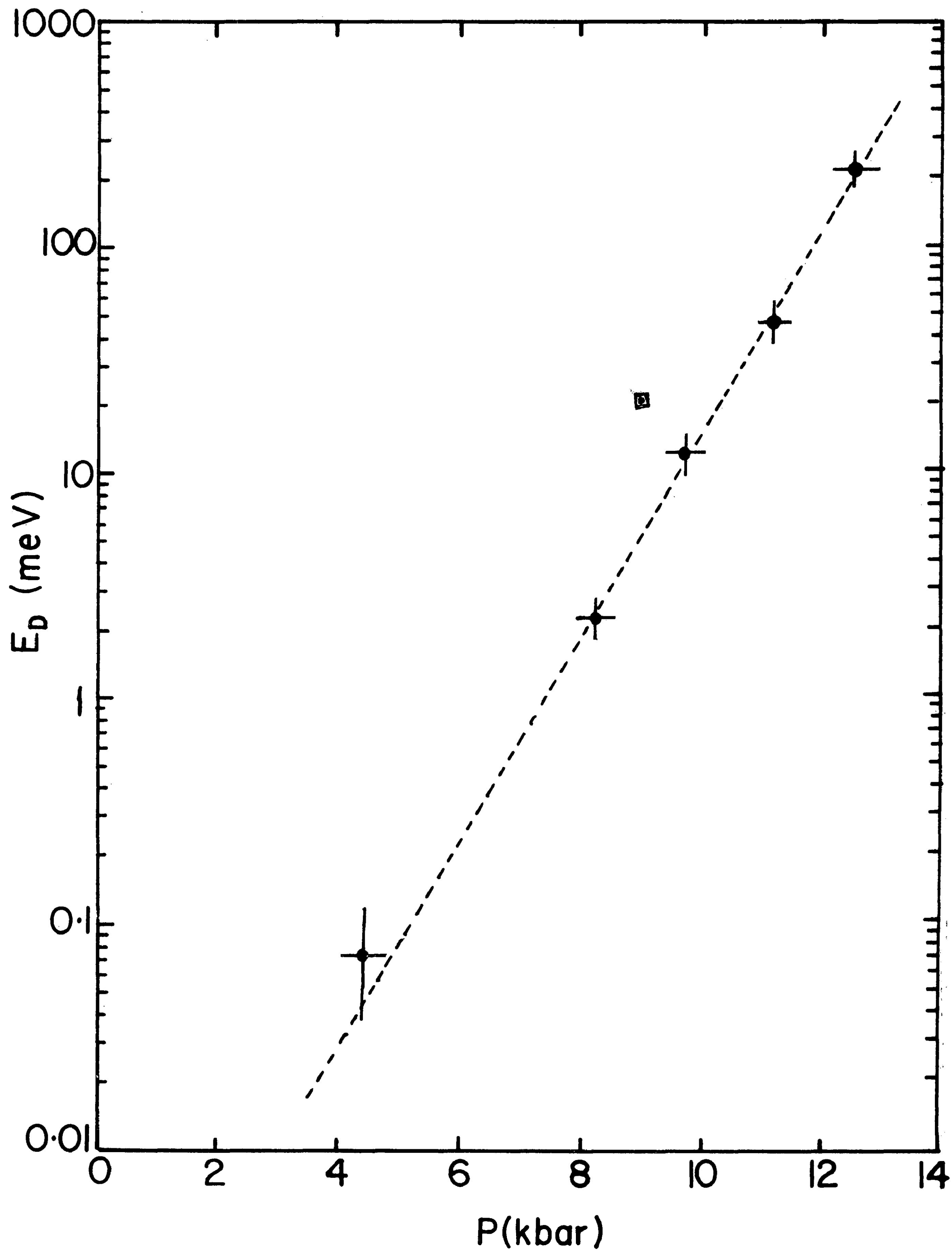

1000
100
10
1
0·1
0·01
0
2
4
6
8
10
12
14
E_D (meV)
P(kbar)

energy levels upward (atomic diamagnetism). However, the unbound conduction band states are also shifted upward, and by a larger amount. Hence the net effect of the magnetic field is to increase the binding energy of the impurity level[24].

Screening[25] of the impurity potential by conduction band electrons is also present when the impurity levels are shallow. This screening decreases the binding energy and for a large enough carrier concentration, the lowest bound state has zero binding energy. Thus, a magnetic field increases the binding energy while screening by conduction band electrons decreases it.

As a magnetic field is increased, the binding energy suddenly increases when the concentration of conduction band electrons drops below the critical concentration for zero binding energy. The process is regenerative because electrons which become bound to impurity ions reduce the number of electrons available for screening and the net result is rapid freeze-out of donor electrons.

It seems reasonable to assume that a similar process is occurring during the pressure freeze-out of carriers. Pressure strongly increases the effective mass of the carriers and hence the orbit size for bound states is reduced. A particular impurity atom is then screened by fewer overlapping impurity electron orbits and again the binding energy should increase since this process is also regenerative. It seems, however, that the degree of freeze-out achievable is much greater using pressure and the effect is measurable

at much higher temperature than in the magnetic case.* The freeze-out process should be sensitive to doping for pressure as it is for the magnetic case since once the impurity number is too large the necessary reduction in screening cannot be accomplished and freeze-out should no longer occur.

Porowski[11] has performed Hall measurements under pressure on similar material to ours and reported an anomalous behavior in R_H as a function of temperature around (90K-140K). We, however, see no such anomaly in ρ vs T for this temperature range and similar pressures (see Fig. 13). We conclude from this that his samples are in some way different from ours. The interesting point, however, is that he calculates a low temperature donor gap E_D of about 20 meV for 9 kbar pressure. This is in reasonable agreement with the 9 meV value obtained during this work.

In a companion experiment we found that the Gunn threshold field $E_{th}(P)$ decreased with increasing pressure and passed through a minimum at about 9 kbar. It then increased and the Gunn oscillations weakened as pressure increased to about 12 kbar. It would appear that the increase in $E_{th}(P)$ for pressures greater than 9 kbar is due to carrier freeze-out caused by the strong pressure dependence of E_D.

*Work is continuing on this effect, and an investigation as a function of donor concentration is in progress. A sample with N_D approximately 10% larger has the pressure induced resistive transition at 77K increased by ~27%. Thus, the "transition" is quite sensitive to donor concentration.

Figure 13. Electrical conductivity $\sigma(T)$ vs $1/T$ for n-InSb at different pressures.

1 : P = 0.2 kbar

2 : P = 2.8 kbar

3 : P = 5.6 kbar

4 : P = 7.5 kbar

5 : P = 9.7 kbar

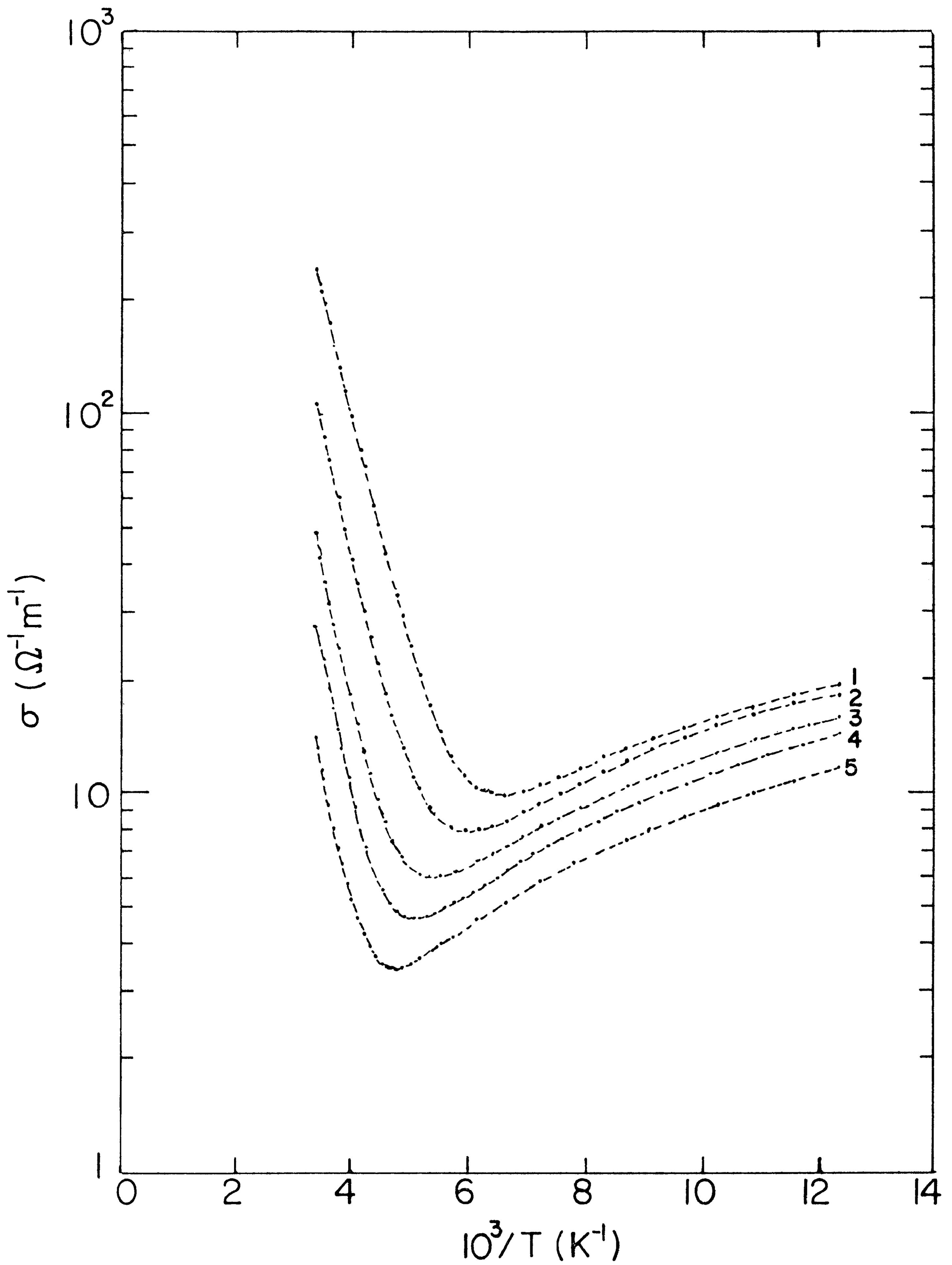

10^3
10^2
10
1
$\sigma\ (\Omega^{-1}m^{-1})$
0
2
4
6
8
10
12
14
$10^3/T\ (K^{-1})$
1
2
3
4
5

$E_{th}(P)$ increases because the field must first ionize the donor atoms before transferring electrons from the Γ to L conduction band. Thus, even though $E_{\Gamma L}$ decreases with increasing pressure, a condition favourable to the Gunn effect, the loss of carriers due to freeze-out more than compensates and the Gunn effect is only seen for higher electric fields as pressure is increased beyond 9 kbar.

3-5. Pressure Dependence of Intrinsic Gap $E_g(P)$

The rate of change of the intrinsic gap with pressure dE_g/dP may be obtained from the plot of n vs P data in Fig. 6a. According to Kane's theory $m_n^* \alpha E_g$, so equation (1-2-5) can be differentiated to give

$$\frac{d\ell nn}{dP} = \frac{3}{4}\frac{d\ell nE_g}{dP} - \frac{1}{2K_BT}\frac{dE_g}{dP}$$

$$= \frac{dE_g}{dP}\left(\frac{3}{4E_g(P)} - \frac{1}{2K_BT}\right)$$

where $E_g(P) = E_g(0) + \frac{dE_g}{dP}\,\delta P$.

Therefore $$\frac{dE_g(P)}{dP} = \frac{d\ell nn}{dP}\left(\frac{3}{4E_g(P)} - \frac{1}{2K_BT}\right)^{-1}$$

Taking $E_g(0) = 0.18$ eV* at P = 0, estimating $d\ell nn/dP$ at P = 0, P = 8 kbar and P = 14 kbar from Fig. 6a and solving for dE_g/dP self-consistently, we obtain

*Accepted zero pressure gap at room temperature.

$$dE_g/dP = 15.5 \pm 0.2 \text{ meV/kbar at } P = 0 \text{ kbar}$$
$$= 13.5 \pm 0.2 \text{ meV/kbar at } P = 8 \text{ kbar}$$
$$= 12.5 \pm 0.1 \text{ meV/kbar at } P = 14 \text{ kbar}$$

Thus dE_g/dP decreases with increasing pressure, in agreement with the ρ vs P curve of Gebbie and Smith[26]. We take as an average value $\frac{dE_g}{dP} = 14.0 \pm 0.2$ meV/kbar.

The zero temperature energy gap $E_{go}(P)$ is obtainable from the slope of a semilog plot of $(n/T^{3/2})$ vs $\frac{1}{T}$ as discussed in section 1-2, equation (1-2-8). Carrier concentration n was determined from Hall measurements for several pressures over the temperature range 305K to 285K. Fig. 14 shows a plot of $E_{go}(P)$ vs P. From this plot we obtain dE_{go}/dP equal to 13.9 ± 0.4 meV/kbar for the 0 to 6 kbar range and 13.0 ± 0.5 meV/kbar from the higher pressure range. These results are in good agreement with the values obtained from the n vs P plot. As before the derivative seems to decrease with increasing pressure. It should be noted that these are constant pressure varying temperature results while the previous results were obtained for constant temperature and varying pressure. Since dE_{go}/dP and dE_g/dP are so close it seems safe to assume that the temperature coefficient α in equation (1-2-7) is insensitive to pressure.

The present values of dE_g/dP and dE_{go}/dP are in good agreement with that of Long[8]. The value of Keyes[9] is somewhat higher at

Figure 14. Intrinsic gap at zero temperature E_{go} vs pressure P for n-InSb.

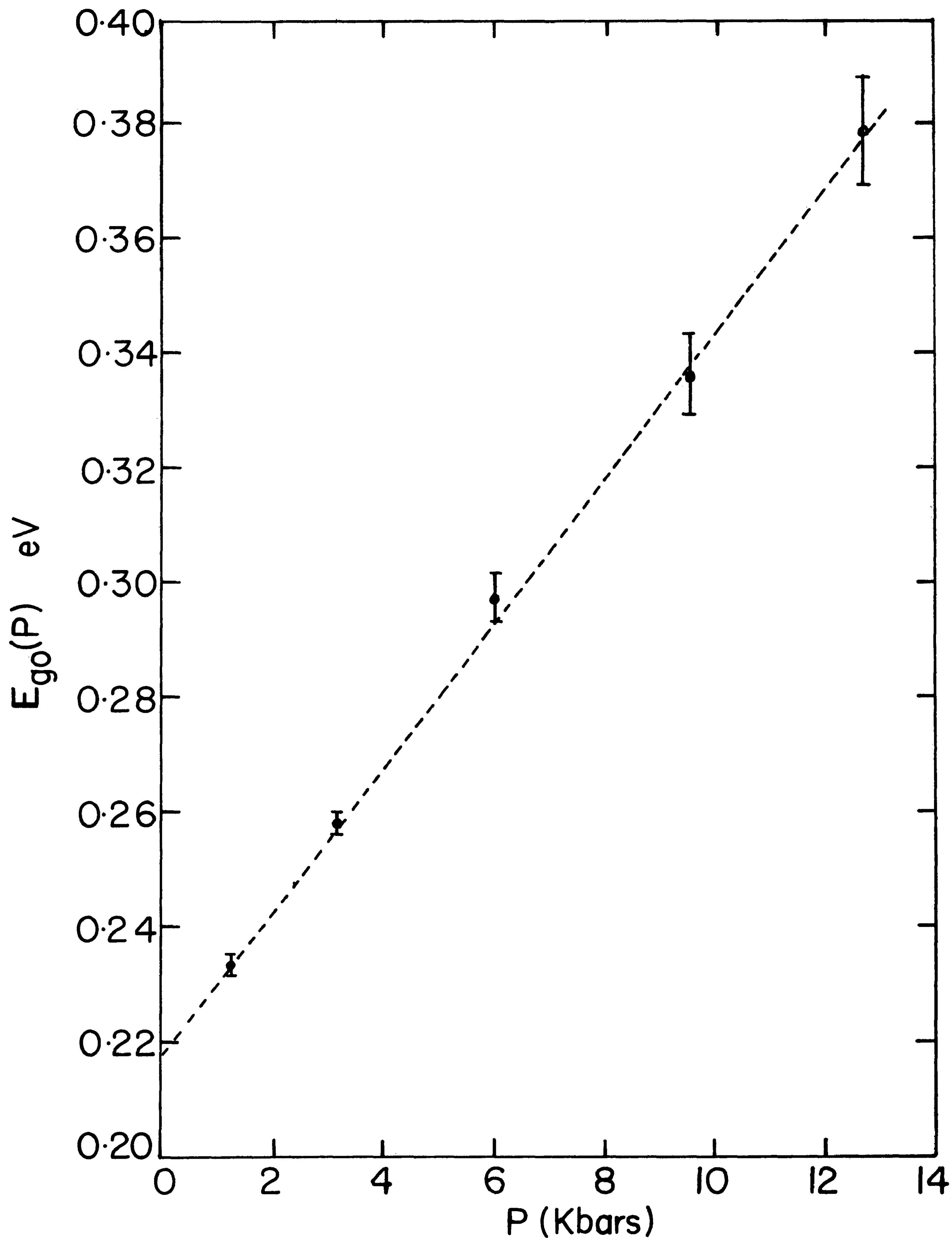
0·40
0·38
0·36
0·34
0·32
0·30
0·28
0·26
0·24
0·22
0·20
$E_{go}(P)$ eV
0
2
4
6
8
10
12
14
P (Kbars)

15.5±1 meV/kbar but is based on resistivity measurements only which means $d\mu/dP$ had to be estimated. In contrast, Long's value was determined using Hall measurements for n and his pressure medium was helium which is very hydrostatic. His result, however, was based on measurements to only 2 kbar. Bradley and Gebbie[27] estimated dE_g/dP at 16±1 meV/kbar using optical absorption. Their result is somewhat higher than the values obtained electrically. In addition, they used solid pyrophyllite as a pressure transmitting medium, hence their result may be influenced by possible non-hydrostatic pressure effects.

Chapter 4

Conclusions

The low electric field transport properties of undoped n-InSb in the temperature range 6.4K-300K have been studied under pressures up to 15 kbar by using Hall measurements.

The measured mobility above 100K (at P = 0) has a $T^{-(1.75\pm0.05)}$ dependence in good agreement with the $T^{-1.7}$ prediction of Ehrenreich[19] which assumes a combination of polar optical and electron-hole scattering. The pressure dependence of the mobility at 296K, 198K and 77K can also be explained assuming these scattering mechanisms.

Below 50K the mobility (at P = 0) has a $T^{0.8}$ dependence and is due to about 85% neutral impurity scattering and 15% ionized impurity scattering. We have used the expressions for the neutral impurity and ionized impurity scattering mobilities to calculate the combined mobility μ_C, $\frac{1}{\mu_C} = \frac{1}{\mu_N} + \frac{1}{\mu_I}$. This gives a $T^{0.8}$ dependence in good agreement with the measured results. The $T^{0.8}$ dependence is due to the temperature dependence in the neutral impurity concentration, N_N, as well as the temperature dependence of $T^{3/2}/n(T)$ in the ionized impurity mobility term. Both of these are close to a $T^{0.8}$ dependence. The importance of μ_N instead of μ_I in determining the magnitude of μ_C is largely due to the small effective mass ratio (m_n^*/m_o) and the way it appears in the two expressions.

For a low impurity concentration, the ionization energy E_D increases approximately exponentially with pressure. In the region of freeze-out, the donor electrons are probably localized to the region of a single impurity atom. For higher donor impurity concentrations the donor electron wave functions probably overlap to higher pressure and a donor band should continue to exist, merged with the conduction band. An investigation of the process of carrier freeze-out as a function of donor concentration is necessary to test this hypothesis.

The pressure dependence of the intrinsic gap E_g also has been determined. The derivative dE_g/dP decreases with increasing pressure. The value of the derivative at 12 kbar is about 10% less than the zero pressure value. The derivative values obtained are in good agreement with those obtained by Long[8] and Keyes[9]. The value of dE_{go}/dP, the derivative at zero temperature, and the value of dE_g/dP, the derivative at room temperature, are so close that it is safe to assume the temperature coefficient α in the expression $E_g = E_{go} - \alpha T$ is pressure independent.

REFERENCES

1. R.J. Sladek, J. Phys. Chem. Solid, 5, p. 157 (1958).

2. L.J. Neuringer, Proc. Ninth Intern. Conf. on Physics of semiconductors, Moscow, 1968, Vol. 2, Nauka, Leningrad (1968), p. 715.

3. H. Miyazawa and H. Ikoma, J. Phys. Soc. Jap., Vol. 23, 290 (1967).

4. R. Mansfield and I. Ahmad, J. Phys. C. Vol. 3, 423 (1970).

5. R. Mansfield, J. Phys. C. Vol. 4, 2084 (1971).

6. E.S. Itskevich and L.M. Kashirskaya, Sov. Phys. Solid State, Vol. 16, No. 10 (1975).

7. M. von Ortenberg, J. Phys. Chem. Solids, Vol. 34, 397 (1973).

8. D. Long, Physical Review, Vol. 99, No. 2, 388 (1955).

9. R.W. Keyes, Physical Review, Vol. 99, No. 2, 490 (1955).

10. M. Konczykowski, S. Porowski and J. Chroboczek, Proc. X1 Intern. Conf. Phys. Semicond. (P.W.N., Warszawa, 1972) Vol. 2, p. 1050.

11. S. Porowski, M. Konczykowski and J. Chroboczek, Phys. Letters, Vol. 48A, No. 3 (1974).

12. E.O. Kane, J. Phys. Chem. Solids, Vol. 1, 249 (1957).

13. S. Porowski and W. Paul, Solid State Communications, Vol. 7, 905 (1969).

14. K. Seeger, Semiconductor Physics, Springer-Verlag (1973), p. 45-46.

15. F. Bardeen and W. Schockley, Phys. Rev., Vol. 77, 407 (1950).

16. H. Ehrenreich, J. Phys. Chem. Solids, Vol. 2, 131 (1957).

17. H.B. Calln, Phys. Rev., Vol. 76, 1394 (1949).

18. H. Ehrenreich, J. Phys. Chem. Solids, Vol. 9, 129 (1959).

19. H. Brook, Advances in Electronics and Electron Phys., Vol. 7, 85 (1955).

20. C. Erginsoy, Phys. Rev., Vol. 79, 1013 (1950).

21. L.J. van der Pauw, Philips Research Reports, Vol. 13, No. 1, (1958).

22. J.C. Phillips, Bonds and Bands in Semiconductors, Academic Press, (1973) p. 94-95.

23. E.W. Fenton and R.R. Haering, Phys. Rev., Vol. 159, No. 3, 593 (1967).

24. Y. Yafet, R.W. Keyes, and E.N. Adams, J. Phys. Chem. Solids, Vol. 1, 137 (1956).

25. C.A. Rouse, Phys. Rev., Vol. 159, No. 1 (1967).

26. H.A. Gebbie, P.L. Smith, I.G. Austin and J.H. King, Nature, Vol. 188, No. 4755 (1960).

27. C.C. Bradley and H.A. Gebbie, Phys. Letters, Vol. 16, No. 2 (1965).